



Contents lists available at ScienceDirect

## Expert Systems With Applications

journal homepage: [www.elsevier.com/locate/eswa](http://www.elsevier.com/locate/eswa)

# Collaborative multiple centers fresh logistics distribution network optimization with resource sharing and temperature control constraints

Yong Wang<sup>a,\*</sup>, Jie Zhang<sup>b</sup>, Xiangyang Guan<sup>c,\*</sup>, Maozeng Xu<sup>a</sup>, Zheng Wang<sup>d</sup>, Haizhong Wang<sup>e</sup>

<sup>a</sup> School of Economics and Management, Chongqing Jiaotong University, Chongqing 400074, China

<sup>b</sup> School of Economics and Management, Southwest Jiaotong University, Chengdu 610031, China

<sup>c</sup> Department of Civil and Environmental Engineering, University of Washington, Seattle, WA 98195, USA

<sup>d</sup> School of Maritime Economics and Management, Dalian Maritime University, Dalian 116026, China

<sup>e</sup> School of Civil and Construction Engineering, Oregon State University, Corvallis, OR 97330, USA

## ARTICLE INFO

## Keywords:

Fresh logistics distribution network  
Collaborative mechanism  
Hybrid heuristic algorithm  
Cost saving  
Profit allocation

## ABSTRACT

Collaboration such as resource sharing among logistics participants (LPs) can effectively increase the efficiency and sustainability of logistics operations, especially in the transportation and distribution of fresh and perishable products that require special infrastructure (e.g., refrigerated trucks/vehicles). This study tackles a collaborative multi-center vehicle routing problem with resource sharing and temperature control constraints (CMCVRP-RSTC). Solving the CMCVRP-RSTC by minimizing the total cost and the number of refrigerated vehicles returns a fresh logistics operational strategy that pinpoints how a multi-center fresh logistics distribution network can be reorganized to highlight potential collaboration opportunities. To find the solution to the CMCVRP-RSTC, we develop a hybrid heuristic algorithm that combines the extended k-means clustering and tabu search non-dominated sorting genetic algorithm-II (TS-NSGA-II) to search a large solution space. This hybrid heuristic algorithm ensures that the optimal solution is found efficiently through initial solution filtering and the combination of local and global searches. Furthermore, we explore how to motivate individual LPs to collaborate by analyzing the benefits of collaboration to each LP. Using the minimum costs remaining savings method and the strictly monotonic path rule, a cost saving calculation model is proposed to find the best profit allocation scheme where each collaborating LP keeps benefiting from long-term collaboration. An empirical case study of Chongqing City, China indicates the efficiency of our proposed collaborative mechanism and optimization algorithms. Our study will help improve the efficiency of logistics operation significantly and contribute to the development of more intelligent logistics systems and smart cities.

## 1. Introduction

The optimization of fresh product logistics networks is always a challenging problem for operators and managers in the cold chain logistics industry. In recent years, the demand for fresh products by urban and rural residents has been increasing. In a 2017 survey, China's fresh product e-commerce transactions reached approximately 140 billion RMB and has been increasing by more than 50%/year, and the loss rate of fresh products has reached 30%/year in the fresh logistics distribution process (Winshang.com, 2018). In addition, the rapid development of on-demand distribution, the ever-increasing consumer demand (Yildiz & Savelsbergh, 2019), and the fact that different fresh product distributions require different temperature control conditions contribute to

the unreasonable vehicle scheduling and facility coordination in the cold chain logistics industry. This trade-off between logistics cost and diversified temperature control conditions increases the difficulty of implementing efficient distribution and vehicle scheduling in fresh product logistics networks. Therefore, properly optimizing the fresh product logistics distribution network and devising a reasonable collaborative mechanism to coordinate multiple facilities have become particularly important for logistics operators.

A collaborative multi-center fresh logistics distribution network (CMFLDN) includes several logistics facilities [e.g., fresh distribution centers (FDCs)] and a large number of customers. In this complicated network, multi-center vehicle routing optimization and the collaborative strategy among fresh logistics facilities should be considered by

\* Corresponding authors.

E-mail addresses: [yongwx@cqjtu.edu.cn](mailto:yongwx@cqjtu.edu.cn) (Y. Wang), [guanxy@uw.edu](mailto:guanxy@uw.edu) (X. Guan), [xmzrzhy@cqjtu.edu.cn](mailto:xmzrzhy@cqjtu.edu.cn) (M. Xu), [drwz@dlut.edu.cn](mailto:drwz@dlut.edu.cn) (Z. Wang), [Haizhong.Wang@oregonstate.edu](mailto:Haizhong.Wang@oregonstate.edu) (H. Wang).

<https://doi.org/10.1016/j.eswa.2020.113838>

Received 20 February 2020; Received in revised form 31 July 2020; Accepted 1 August 2020

Available online 9 August 2020

0957-4174/© 2020 Elsevier Ltd. All rights reserved.

logistics enterprises. The ultimate goal of CMFLDN optimization is to minimize the total logistics operation cost and the number of refrigerated vehicles used in fresh logistics distribution networks (FLDNs). The cold chain infrastructure is generally insufficient in existing fresh logistics networks. For example, the number of refrigerated trucks accounts for only 0.3% of the total number of trucks in China, while that of Japan reaches 2% (China.com, 2016). Independent and complete cold chain logistics transportation systems have not been established. For example, the *trans*-provincial transportation of fresh products is mostly normal-temperature transportation. Given the limited capacity of current fresh logistics facilities, resource sharing among fresh logistics facilities through collaboration has become a critical issue in FLDNs. Typically, a third-party logistics service provider (LSP) or one of the collaborative alliance members is responsible for coordinating the logistics facilities in collaboration and developing appropriate collaboration strategies for the alliance members (Wang et al., 2017a; Lin & Chang, 2018). This practice optimizes the logistics operations in a CMFLDN, effectively reduces the total cost, improves the distribution efficiency of fresh products, and reduces the loss due to product perishing during transportation.

This paper formulates and solves the collaborative multi-center vehicle routing problem with resource sharing and temperature control constraints (CMCVRP-RSTC), in which the distribution and delivery of fresh products can be coordinated among multiple FDCs via a collaborative optimization network framework (Lee & Jeong, 2009; Özen et al., 2012; Schmitt et al., 2015). In addition, resource sharing and temperature control constraints are considered in the problem to facilitate the rational use of resources and reduce logistics operation costs. Integrating these two constraints also helps the third-party LSP coordinate logistics operations better (Abbasi & Nilsson, 2016; Centobelli et al., 2017; Fernández et al., 2018), including the sharing of refrigerated vehicles during different service periods and the balance between temperature control and loss of value. To optimize the CMCVRP-RSTC, we first design a bi-objective mixed-integer linear model that minimizes the total logistics costs and the number of refrigerated vehicles. A customer clustering procedure is then employed to assign customers into different logistics facilities for service (Liu & Zhang, 2017; Wang, 2018). Then, a composite algorithm is developed to reduce the complexity of fresh distribution network optimization, facilitating the search for the near-best route for the CMCVRP-RSTC. Finally, a profit allocation strategy based on cooperative game theory is proposed to allocate profit among the collaborative participants in the CMFLDN.

The remainder of this paper is organized as follows. In Section 2, related studies are reviewed and summarized. In Section 3, the problem description and a bi-objective optimization model formulation of the CMCVRP-RSTC are presented. In Section 4, a composite algorithm for solving the optimization, including an extended k-means clustering algorithm and a hybrid heuristic algorithm consisting of tabu search (TS) and NSGA-II, is described. Then, a model for calculating the minimum costs remaining savings (MCRS) with different collaborative participants is introduced to allocate profits fairly. In Section 5, an empirical study of the CMFLDN optimization in Chongqing City, China is presented and used to evaluate the effectiveness of the proposed model and algorithm. In Section 6, conclusions and future work are summarized and discussed.

## 2. Literature review

With the advent of the big data era and new technology, the optimization of CMFLDNs has become increasingly important and feasible. However, traditional approaches cannot deal with complex FLDNs effectively. Owing to the perishability of fresh products, the heterogeneous quality decay and time dependent value loss of fresh products should be considered in the optimization of CMFLDNs, such as vehicle routing problems based on the minimum logistics operational cost and value loss of perishable food (Chen et al., 2009; Amorim & Almada-

Lobo, 2014; Wang et al., 2016), time-dependent vehicle routing problems with the minimum total heterogeneous fleet cost (Behrouz & Alireza, 2017; Hu et al., 2017), and vehicle scheduling problems for perishable products including the travel time of vehicles and the freshness of products (Keizer et al., 2017; Rahbari et al., 2019). These previous studies inspire us to introduce heterogeneous product quality decay, travel time, and logistics operating cost into the CMCVRP to improve the operational efficiency of CMFLDNs.

A certain similarity exists between the CMCVRP-RSTC and the multi-depot vehicle routing problem with time windows (MDVRPTW). As an extension of MDVRPTW, resource sharing and temperature control constraints are further studied in the CMCVRP-RSTC (Li et al., 2016; Yu et al., 2017; Stellingwerf et al., 2018). Ju & Mu (2010) established a logistics service model based on a multi-temperature joint distribution system, providing a new scenario for the distribution and storage of multi-temperature-controlled products. Hsu & Liu (2011) proposed a multi-temperature joint distribution system, and achieved precise multi-temperature control logistics technology and food handling capacity to maximize costs and mitigate the negative impact of extreme temperatures on food quality. For years, the combination of the integer programming model and the hybrid heuristic algorithm has been used often to study the MDVRPTW under shared depot resources (Li et al., 2016), and address the cold chain perishable food distribution planning problem with multi-item-multi-temperature vehicles (Yu et al., 2017). In addition, several extended problems have been used as references of fresh logistics distribution problems. For instance, Stellingwerf et al. (2018) developed an extension of the load-dependent vehicle routing problem model to study the temperature-controlled fresh food transportation problem. Wang et al. (2019) proposed a transportation resource sharing strategy to study the multi-depot green vehicle routing problem, including time-dependent speed and piecewise penalty cost.

Customer clustering is performed according to attribute characteristics, such as the time window requirements, the spatial location of customers, the temperature control conditions of fresh products, and customer demands. With proper customer clustering approaches, a large-scale multiple centers logistics distribution network can be decomposed into small zones, and the vehicle routing problem can be further optimized within each small zone (Chen et al., 2012; Wang et al., 2014, 2018a; Mesa-Arango & Ukkusuri, 2015). In addition, the time-space based clustering method is often extended to study the features of customer behaviors and various types of logistics services (Liu & Zhang, 2017; Wang, 2018). However, although clustering methods can reduce computational complexity (Kuo et al., 2016; Wang et al., 2019b), heuristic or combined heuristic algorithms show a high computational speed in solving the MDVRPTW and complicated problems in related fields (Narasimha et al., 2013; Song & Ko, 2016). For example, Ma et al. (2017) presented a hybrid ant colony algorithm consisting of local search operators to study the time-dependent vehicle routing problem for perishable product delivery. Li et al. (2018) proposed a hybrid genetic algorithm with adaptive local search to study the benefit of shared depot resources for MDVRPs. Diabat et al. (2019) established a bi-objective robust optimization model and devised a solution algorithm based on Lagrangian relaxation and the  $\epsilon$ -constraint to investigate the impacts of disruptions on a perishable product supply chain network.

The CMCVRP-RSTC optimization process usually involves multi-depot vehicle routing optimization and the problem of collaborative mechanism design. The coalition sequence and profit allocation relationship among players can be used for analysis in collaborative mechanism design (Hellström et al., 2015; Lai et al., 2017). Nguyen et al. (2014) presented a proportional cost allocation scheme among suppliers to study the delivery of perishable products based on freight consolidation strategies. However, the advantages of sharing economy motivate the formulation of coalitions based on the core stability and equilibrium strength in collaborative logistics operations (Guajardo & Rönnqvist, 2015; Kimms & Kozeletskyi, 2016). Furthermore, related research includes information resource sharing (Özener et al., 2011),

collaborative stability with transportation consolidation (Lai et al., 2017), coalition sequence rules for multi-echelon supply chains (Liu & Papageorgiou, 2018), and fair profit allocation schemes for coalition formulation among participants (Fahimullah et al., 2019).

However, previous research has encountered the following issues. (1) The timeliness and temperature control requirements in fresh product distribution have not been sufficiently accounted for, especially in collaborative fresh logistics networks. (2) Gaps exist in the study of resource sharing in CMFLDNs, that is, previous research did not consider the sharing of facilities and vehicles among multiple FDCs. The effect of resource sharing on the value loss of fresh products and the logistics cost is largely unexplored. (3) Collaborative mechanisms have constantly been overlooked by existing studies, which assume that collaboration is facilitated through external forces (e.g., government incentives). How collaborative alliances motivated by the benefit of collaboration itself could form in CMFLDNs, and how stable are these alliances remain important unanswered questions.

The main contribution of this research is the development of an optimization modeling framework for collaborative FLDNs, which addresses the three limitations of existing studies. (1) FDC and customer service time windows, temperature control requirements, resource sharing, and collaborative mechanisms are simultaneously incorporated in this modeling framework to formulate a holistic fresh product distribution problem in a realistic setting. (2) A novel solution algorithm for this optimization problem is also proposed and tested, which outperforms existing solution algorithms. (3) A collaborative mechanism on the basis of the MCRS model and the SMP rule is developed to study the collaborative coalition sequences in CMFLDNs, sensitivity analysis is performed under different temperature conditions based on the Pareto-optimal principle, and the effectiveness of the proposed model and approach is evaluated in a real-world case study. Therefore, this study marks a significant advance in the state of practice of the fresh logistics industry.

### 3. Problem statement and mathematical model

#### 3.1. Problem statement

The recent surge of on-demand delivery of fresh products has strained logistics facilities and distribution resources. The CMCVRP-RSTC integrates and optimizes resource sharing and temperature control to handle the CMCVRP of fresh products. The CMFLDN involves several FDCs and a certain number of customers. Each FDC has its own service area and customers. Each FDC also has a fixed number of identical refrigerated vehicles, and can run multiple delivery routes during the planned service time periods. To effectively control the logistics cost of fresh product distribution, the CMCVRP-RSTC comprehensively considers the collaboration among multiple centers and the temperature control constraints of fresh products to optimize resource utilization and reduce the total operating cost.

Different types of fresh products have different temperature control constraints and customer service time windows. A non-collaborative FLDN example is shown in Fig. 1, where each FDC must serve customers whose orders have similar temperature control requirements. Customer demands are served ineffectively in this non-collaborative network structure due to crisscross and long-distance transportation. Therefore, the collaboration among multiple FDCs and the sharing of resources, such as logistics facilities, customer services, and vehicles must be optimized in this non-collaborative FLDN structure. The optimized CMFLDN is shown in Fig. 2.

As shown in Fig. 2, the operating hours of each FDC in the CMFLDN is divided into multiple service time periods to facilitate resource sharing and operation scheduling. Transshipping of fresh products among FDCs due to merged customer demands can be carried out by a fleet of refrigerated trucks. The optimization of the CMCVRP-RSTC aims to optimally serve customers under time window and temperature control constraints. Several key issues should be addressed when transitioning from a non-collaborative to a collaborative network: 1) the design of an optimal network structure with resource sharing in CMFLDN; 2) balance of the value loss of fresh products and the logistics operation cost; and 3) develop of a collaborative mechanism to allocate the benefits of

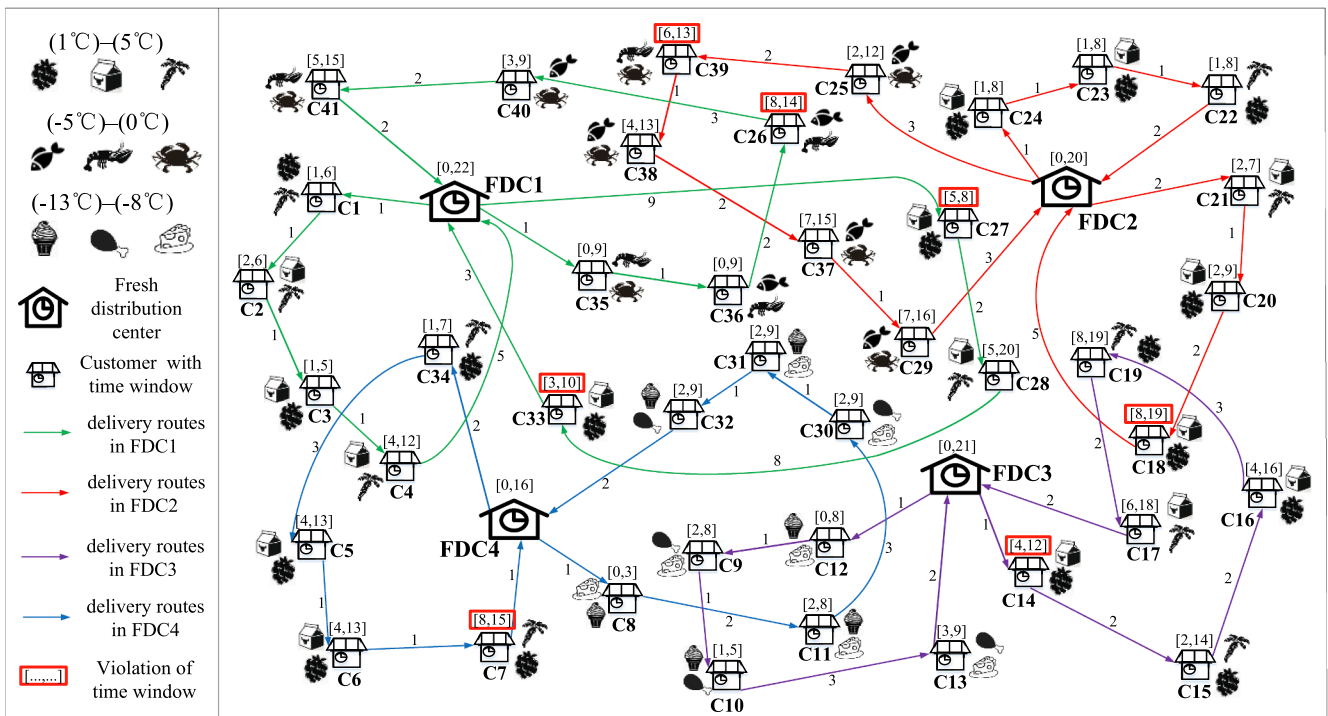


Fig. 1. Non-collaborative FLDN.

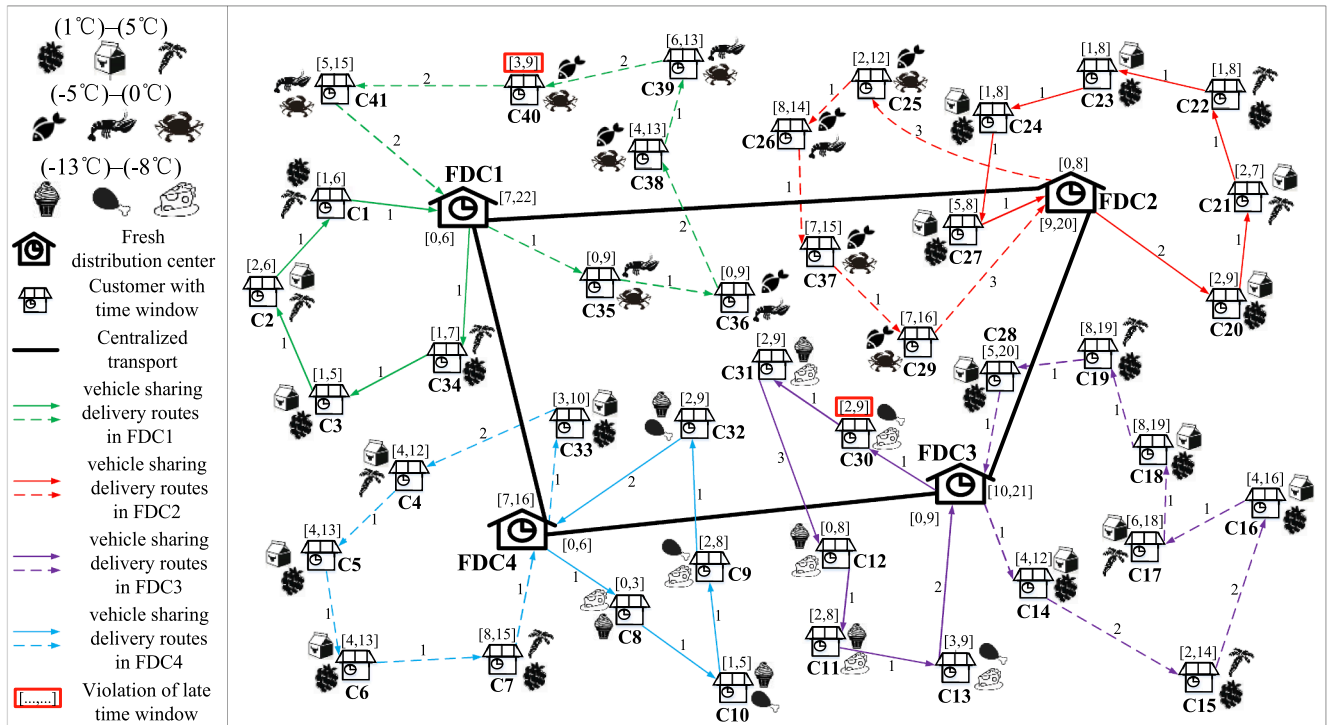


Fig. 2. Collaborative FLDN.

collaboration.

For each temperature control range (TCR), the temperature control cost (TCC) and value loss (VL) at different temperatures are shown in Table 1. For example, the TCCs are \$15 and \$18 per unit time for 0 °C and -3 °C, respectively in the temperature control range (-5 °C)-(0 °C). The total logistics operational cost (TLOC) includes the distribution cost (DCO), the penalty cost (PC), and the collaborative cost (CC). We assume that the transportation cost is \$20 per unit time, and the PC (earliness and delay penalties) is \$30 per unit time. The comparison of delivery time, TLOC, and number of vehicles before and after optimization is shown in Table 2. Significant decreases in the TLOC, the number of vehicles, and the total delivery time can be observed through an effective collaborative mechanism and a reasonable temperature control design.

### 3.2. Model formulation for the CMCVRP-RSTC optimization

Some of the notations and definitions used to formulate the CMCVRP-RSTC optimization model are shown in Table 3.

The optimization of the CMCVRP-RSTC is formulated as a bi-objective model aiming at minimizing the total cost and the number of refrigerated vehicles, where the total cost consists of the transportation cost, the TCC, the PC, and the VL. These costs are explained in

detail in the remainder of this section.

The transportation cost ( $TC_1$ ) consists of the following components:  $\sum_{i,j \in N \cup I, i \neq j} \sum_{v \in V} \sum_{\pi \in \Pi} \sum_{w \in W} (x_{ijvw}^{\pi} \cdot \beta_{ij} \cdot f_{vw} \cdot \sigma_q)$  is the DCO of fresh products from FDCs to customers,  $\sum_{n,a \in N, n \neq a} \sum_{k \in K} \sum_{w \in W} \sum_{\pi \in \Pi} [Z_{nakw}^{\pi} \cdot \beta_{na} \cdot (f_{kw} \cdot B_{naw}) \cdot \sigma_c]$  is the centralized transportation cost of refrigerated trucks among FDCs, and  $CR_n \cdot \gamma_n \cdot IC_n$  expresses the cost reduction considering the discount from LSP incentives.

$$TC_1 = \left\{ \begin{array}{l} \sum_{i,j \in N \cup I, i \neq j} \sum_{v \in V} \sum_{\pi \in \Pi} \sum_{w \in W} (x_{ijvw}^{\pi} \cdot \beta_{ij} \cdot f_{vw} \cdot \sigma_q) + \\ \sum_{n,a \in N, n \neq a} \sum_{k \in K} \sum_{w \in W} \sum_{\pi \in \Pi} [Z_{nakw}^{\pi} \cdot \beta_{na} \cdot (f_{kw} \cdot B_{naw}) \cdot \sigma_c] + CR_n \cdot \gamma_n \cdot IC_n \end{array} \right\} \quad (1)$$

The TCC ( $TC_2$ ) includes the following components:  $\sum_{i,j \in N \cup I, i \neq j} \sum_{v \in V} \sum_{m \in M} \sum_{\pi \in \Pi} \sum_{w \in W} (ct_{ijv}^{\pi w} \cdot g_{mw} \cdot q_{ijv\pi}^{mw})$  is the TCC for refrigerated vehicles to deliver fresh products from FDCs to customers, and  $\sum_{n,a \in N, n \neq a} \sum_{k \in K} \sum_{m \in M} \sum_{\pi \in \Pi} \sum_{w \in W} (ct_{nak}^{\pi w} \cdot g_{mw} \cdot q_{nak\pi}^{mw})$  is the TCC for refrigerated trucks to transport fresh products among FDCs.

$$TC_2 = \left\{ \begin{array}{l} \sum_{i,j \in N \cup I, i \neq j} \sum_{v \in V} \sum_{m \in M} \sum_{\pi \in \Pi} \sum_{w \in W} (ct_{ijv}^{\pi w} \cdot g_{mw} \cdot q_{ijv\pi}^{mw}) + \\ \sum_{n,a \in N, n \neq a} \sum_{k \in K} \sum_{m \in M} \sum_{\pi \in \Pi} \sum_{w \in W} (ct_{nak}^{\pi w} \cdot g_{mw} \cdot q_{nak\pi}^{mw}) \end{array} \right\} \quad (2)$$

Table 1

VL and TCC with different temperature control ranges.

TCR	Temperature	TCC	VL	TCR	Temperature	TCC	VL
(-13 °C)-(-8 °C)	-13 °C	\$28	\$7	(-5 °C)-(0 °C)	-5 °C	\$20	\$5
	-12 °C	\$27	\$8		-4 °C	\$19	\$6
	-11 °C	\$26	\$9		-3 °C	\$18	\$7
	-10 °C	\$25	\$10		-2 °C	\$17	\$8
	-9 °C	\$24	\$11		-1 °C	\$16	\$9
	-8 °C	\$23	\$12		0 °C	\$15	\$10
(1 °C)-(3 °C)	1 °C	\$18	\$6	(4 °C)-(5 °C)	4 °C	\$15	\$9
	2 °C	\$17	\$7		5 °C	\$14	\$10
	3 °C	\$16	\$8				

**Table 2**  
Comparison before and after collaboration.

Case	DCO (\$)	PC (\$)	CC (\$)	TCC(\$)	VL (\$)	TLOC (\$)	Number of vehicles	Total delivery time
Before collaboration	2140	660	0	1683	1106	5589	10	107
After collaboration	1300	180	400	1245	500	3625	4	65

The PC ( $TC_3$ ) consists of the following components:  $\sum_{i \in I} \sum_{\pi \in \Pi} \sum_{m \in M} \sum_{w \in W} \sum_{v \in V} \psi_{m1} \cdot D_{im\pi}^w \cdot [\max\{e_{ix} - rt_{ix}^v, 0\}]$  and  $\sum_{i \in I} \sum_{\pi \in \Pi} \sum_{m \in M} \sum_{w \in W} \sum_{v \in V} \psi_{m2} \cdot D_{im\pi}^w \cdot [\max\{rt_{ix}^v - li\pi, 0\}]$  are the PCs of the earliness and delay of refrigerated vehicles in delivering fresh products to customers, respectively.  $\sum_{n,a \in N, n \neq a} \sum_{\pi \in \Pi} \sum_{m \in M} \sum_{w \in W} \sum_{k \in K} \psi_{m1} \cdot S_{nam}^{w\pi} \cdot [\max\{e_{ax} - rt_{ax}^k, 0\}]$  and  $\sum_{n,a \in N, n \neq a} \sum_{\pi \in \Pi} \sum_{m \in M} \sum_{w \in W} \sum_{k \in K} \psi_{m2} \cdot S_{nam}^{w\pi} \cdot [\max\{rt_{ax}^k - l_{ax}, 0\}]$  are the PCs for earliness and delay for refrigerated trucks in transporting fresh products among the FDCs, respectively.

$$ht_{n\pi}^v + ct_{niv}^{\pi w} + RR(1 - x_{nivw}^{\pi}) \geq rt_{ix}^v, \quad \forall n, i, j \in N \cup I, \forall v \in V, \forall w \in W, \forall \pi \in \Pi \quad (13)$$

$$ht_{n\pi}^k + ct_{nak}^{\pi w} - RR(1 - Z_{nakw}^{\pi}) \leq rt_{ax}^k, \quad \forall n, a \in N, n \neq a, \forall k \in K, \forall w \in W, \forall \pi \in \Pi \quad (14)$$

$$ht_{n\pi}^k + ct_{nak}^{\pi w} + RR(1 - Z_{nakw}^{\pi}) \geq rt_{ax}^k, \quad \forall n, a \in N, n \neq a, \forall k \in K, \forall w \in W, \forall \pi \in \Pi \quad (15)$$

$$TC_3 = \left\{ \begin{aligned} & \sum_{i \in I} \sum_{\pi \in \Pi} \sum_{m \in M} \sum_{w \in W} \sum_{v \in V} \psi_{m1} \cdot D_{im\pi}^w \cdot [\max\{e_{ix} - rt_{ix}^v, 0\}] + \sum_{i \in I} \sum_{\pi \in \Pi} \sum_{m \in M} \sum_{w \in W} \sum_{v \in V} \psi_{m2} \\ & \cdot D_{im\pi}^w \cdot [\max\{rt_{ix}^v - li\pi, 0\}] + \sum_{n,a \in N, n \neq a} \sum_{\pi \in \Pi} \sum_{m \in M} \sum_{w \in W} \sum_{k \in K} \psi_{m1} \cdot S_{nam}^{w\pi} \cdot [\max\{e_{ax} - rt_{ax}^k, 0\}] \\ & + \sum_{n,a \in N, n \neq a} \sum_{\pi \in \Pi} \sum_{m \in M} \sum_{w \in W} \sum_{k \in K} \psi_{m2} \cdot S_{nam}^{w\pi} \cdot [\max\{rt_{ax}^k - l_{ax}, 0\}] \end{aligned} \right\} \quad (3)$$

The VL ( $TC_4$ ) consists of the following two components:  $\sum_{\pi \in \Pi} \sum_{i \in I} \sum_{m \in M} \sum_{w \in W} \sum_{v \in V} \sum_{n \in N} r_{iw}^{m\pi} \cdot (1 - \xi_w^m \cdot ct_{niv}^{\pi w}) \cdot D_{im\pi}^w \cdot p_m$  and  $\sum_{\pi \in \Pi} \sum_{n,a \in N, n \neq a} \sum_{m \in M} \sum_{w \in W} \sum_{k \in K} r_{aw}^{m\pi} \cdot (1 - \xi_w^m \cdot ct_{nak}^{\pi w}) \cdot S_{nam}^{w\pi} \cdot p_m$  are the VLs of perished fresh products in the process of delivery from the FDCs to the customers and transportation among FDCs, respectively.

$$\sum_{i,j \in I, i \neq j} \sum_{v \in V} \sum_{w \in W} x_{ijvw}^{\pi} = |I_{nv\pi}| - 1, \quad \forall I_{nv\pi} \subseteq I \quad (16)$$

$$\sum_{\pi \in \Pi} \sum_{v \in V} \sum_{w \in W} y_{ivw}^{\pi} = 1, \quad \forall i \in I \quad (17)$$

$$\sum_{i \in N \cup I} \sum_{j \in I} x_{ijvw}^{\pi} \leq 1, \quad \forall v \in V, \forall \pi \in \Pi \quad (18)$$

$$\sum_{i \in N \cup I} \sum_{w \in W} x_{ijvw}^{\pi} - \sum_{i \in N \cup I} \sum_{w \in W} x_{ijvw}^{\pi} = 0, \quad \forall j \in I, \forall v \in V, \forall \pi \in \Pi \quad (19)$$

$$\sum_{i \in N \cup I} x_{ijvw}^{\pi} = y_{jvw}^{\pi}, \quad \forall j \in I, \forall v \in V, \forall w \in W, \forall \pi \in \Pi \quad (20)$$

$$\sum_{j \in N \cup I} x_{ijvw}^{\pi} = y_{ivw}^{\pi}, \quad \forall i \in I, \forall v \in V, \forall w \in W, \forall \pi \in \Pi \quad (21)$$

$$e_{ax} \leq ht_{n\pi}^v \leq l_{ax} \quad (22)$$

$$\sum_{i \in N \cup I} \sum_{j \in I} ct_{ijv}^{\pi w} \leq T_{max}, \quad \forall v \in V, \forall w \in W, \forall \pi \in \Pi \quad (23)$$

$$TC_4 = \left\{ \begin{aligned} & \sum_{\pi \in \Pi} \sum_{i \in I} \sum_{m \in M} \sum_{w \in W} \sum_{v \in V} \sum_{n \in N} r_{iw}^{m\pi} \cdot (1 - \xi_w^m \cdot ct_{niv}^{\pi w}) \cdot D_{im\pi}^w \cdot p_m + \\ & \sum_{\pi \in \Pi} \sum_{n,a \in N, n \neq a} \sum_{m \in M} \sum_{w \in W} \sum_{k \in K} r_{aw}^{m\pi} \cdot (1 - \xi_w^m \cdot ct_{nak}^{\pi w}) \cdot S_{nam}^{w\pi} \cdot p_m \end{aligned} \right\} \quad (4)$$

In Eq. (5), the total cost ( $F_1$ ) includes the transportation cost, the TCC, the PC, and the VL. Eq. (6) derives the minimum number of refrigerated vehicles ( $F_2$ ) when resource sharing in multiple service time periods is considered.

$$F_1 = \min\{TC_1 + TC_2 + TC_3 + TC_4\} \quad (5)$$

$$F_2 = \max_{\pi \in \Pi} \left\{ \min_{v \in V} y_v^{\pi} \cdot \min \left\{ \sum_{n \in N} \sum_{i \in I} \sum_{w \in W} x_{nivw}^{\pi}, 1 \right\} \right\} \quad (6)$$

Subject to

$$\sum_{i \in N \cup I} \sum_{m \in M} \sum_{w \in W} y_{ivw}^{\pi} \cdot D_{im\pi}^w \leq Q_v, \quad \forall v \in V, \forall \pi \in \Pi \quad (7)$$

$$\sum_{n,a \in N, n \neq a} \sum_{m \in M} \sum_{w \in W} Z_{nakw}^{\pi} \cdot S_{nam}^{w\pi} \leq Q_k, \quad \forall k \in K, \forall \pi \in \Pi \quad (8)$$

$$\sum_{w \in W} S_{nam}^{w\pi} = \sum_{i \in I} \sum_{w \in W} Z_{nia}^{\pi} \cdot D_{im\pi}^w, \quad \forall n, a \in N, n \neq a, \forall \pi \in \Pi \quad (9)$$

$$rt_{jn}^v = rt_{in}^v + ct_{ijv}^{\pi w}, \quad \forall i, j \in N \cup I, i \neq j, \forall v \in V, \forall w \in W, \forall \pi \in \Pi \quad (10)$$

$$rt_{ax}^k = rt_{n\pi}^k + ct_{nak}^{\pi w}, \quad \forall n, a \in N, n \neq a, \forall k \in K, \forall w \in W, \forall \pi \in \Pi \quad (11)$$

$$ht_{n\pi}^v + ct_{niv}^{\pi w} - RR(1 - x_{nivw}^{\pi}) \leq rt_{ix}^v, \quad \forall n, i \in N \cup I, \forall v \in V, \forall w \in W, \forall \pi \in \Pi \quad (12)$$

**Table 3**  
Notations and definitions in CMCVRP-RSTC optimization.

Symbol	Definition
<b>Sets</b>	
$N$	Set of FDCs, $N = \{n n = 1, 2, 3, \dots, a\}$
$\Pi$	Set of service time periods, $\Pi = \{\pi \pi = 1, 2, 3, \dots, g\}$
$I$	Set of customers, $I = \{i i = 1, 2, 3, \dots, j\}$
$M$	Set of product categories, $M = \{m m = 1, 2, 3, \dots, c\}$
$K$	Set of refrigerated trucks, $K = \{k k = 1, 2, 3, \dots, d\}$
$W$	Set of temperature control ranges, $W = \{w w = 1, 2, 3, \dots, f\}$
$V$	Set of refrigerated vehicles, $V = \{v v = 1, 2, 3, \dots, e\}$
$V_\pi$	Set of refrigerated vehicles for serving customers within the $\pi$ th service time period, $\pi \in \Pi$
$I_{nv\pi}$	Set of customers served by refrigerated vehicle $v$ from FDC $n$ within the $\pi$ th service time period, $n \in N, v \in V, \pi \in \Pi$
<b>Parameters</b>	
$\beta_{ij}$	Distance between customers $i$ and $j$ in the logistics distribution network
$\beta_{na}$	Distance between FDCs $n$ and $a$
$D_{im}^w$	Demand of customer $i$ for fresh product $m$ at temperature $w$ within the $\pi$ th service time period
$\psi_{m1}$	Penalty factor per time unit of earliness for per unit fresh product $m$
$\psi_{m2}$	Penalty factor per time unit of delay for per unit fresh product $m$
$S_{nam}^w$	Transport quantity of fresh product $m$ from FDC $n$ to $a$ at temperature $w$ within the $\pi$ th service time period
$p_m$	Unit value of fresh product $m$
$Q_k$	Capacity of refrigerated truck $k$
$Q_v$	Capacity of refrigerated vehicle $v$
$\xi_w^m$	Coefficient of freshness degradation over time for fresh product $m$ at temperature $w$
$f_{vw}$	Average fuel consumption of refrigerated vehicle $v$ per 100 miles at temperature $w$
$f_{kw}$	Average fuel consumption of refrigerated truck $k$ per 100 miles at temperature $w$
$c_{ijv}^{\pi w}$	Travel time of refrigerated vehicle $v$ from customer $i$ to $j$ at temperature $w$ within the $\pi$ th service time period
$c_{niv}^{\pi w}$	Travel time of refrigerated vehicle $v$ from FDC $n$ to customer $i$ at temperature $w$ within the $\pi$ th service time period
$c_{nak}^{\pi w}$	Transport time of refrigerated truck $k$ from FDC $n$ to $a$ at the temperature $w$ within the $\pi$ th service time period
$g_{mw}$	Temperature control cost per unit fresh product $m$ per time unit at temperature $w$
$rt_{iv}^v$	Arrival time of refrigerated vehicle $v$ at customer $i$ within the $\pi$ th service time period
$rt_{ax}^k$	Arrival time of refrigerated truck $k$ at FDC $a$ within the $\pi$ th service time period
$ht_{nv}^v$	Departure time of refrigerated vehicle $v$ from FDC $n$ within the $\pi$ th service time period
$ht_{nk}^k$	Departure time of refrigerated truck $k$ from FDC $n$ within the $\pi$ th service time period
$\sigma_q$	Gasoline price (dollars/gallon)
$\sigma_c$	Diesel price (dollars/gallon)
$\gamma_n$	Incentive provided to FDC $n$ by LSP
$IC_n$	Initial independent operational cost of FDC $n$ with non-collaboration
$[e_{iv}, l_{iv}]$	Service time window of customer $i$ within the $\pi$ th service time period
$[e_{ax}, l_{ax}]$	Service time window of FDC $a$ within the $\pi$ th service time period
$ I_{nv\pi} $	Number of customers served by refrigerated vehicle $v$ from FDC $n$ within the $\pi$ th service time period
$q_{ijv}^{mw}$	Quantity of fresh product $m$ at temperature $w$ on refrigerated vehicle $v$ en route from customer $i$ to $j$ within the $\pi$ th service time period
$q_{nak}^{mw}$	Quantity of fresh product $m$ at temperature $w$ on refrigerated truck $k$ en route for transport from FDC $n$ to $a$ within the $\pi$ th service time period
$RR$	A large enough positive integer
$Tmax$	Maximum en-route time allowed for a vehicle
<b>Decision variables</b>	
$Z_{nak}^\pi$	Equal to 1 if refrigerated truck $k$ transports directly from FDC $n$ to $a$ at temperature $w$ within the $\pi$ th service time period, and 0 otherwise
$Z_{nak}^\pi$	Equal to 1 if customer $i$ is reassigned from FDC $n$ to $a$ within the $\pi$ th service time period, and 0 otherwise
$B_{nak}^\pi$	Equal to 1 if temperature control range is $w$ from FDC $n$ to $a$ , and 0 otherwise

**Table 3 (continued)**

Symbol	Definition
$x_{ijvw}^\pi$	Equal to 1 if refrigerated vehicle $v$ travels directly from customer $i$ to $j$ at temperature $w$ within the $\pi$ th service time period, and 0 otherwise
$x_{ijvw}^\pi$	Equal to 1 if refrigerated vehicle $v$ travels directly from DC $n$ to customer $i$ at temperature $w$ within the $\pi$ th service time period, and 0 otherwise
$r_{iw}^{m\pi}$	Equal to 1 if fresh product $m$ is delivered to customer $i$ at temperature $w$ within the $\pi$ th service time period
$r_{aw}^{m\pi}$	Equal to 1 if fresh product $m$ is transported to FDC $a$ at temperature $w$ within the $\pi$ th service time period
$y_{ivw}^\pi$	Equal to 1 if customer $i$ is served by refrigerated vehicle $v$ at temperature $w$ within the $\pi$ th service time period, and 0 otherwise
$y_{jvw}^\pi$	Equal to 1 if customer $j$ is served by refrigerated vehicle $v$ at temperature $w$ within the $\pi$ th service time period, and 0 otherwise
$y_{v\pi}^\pi$	Equal to 1 if refrigerated vehicle $v$ is selected for a delivery task within the $\pi$ th service time period, and 0 otherwise
$CR_n$	Equal to 1 if FDC $n$ agrees to collaborate with LSP, and 0 otherwise

Constraint (7) stipulates that the sum of customer demands on a single delivery route cannot exceed the capacity of each refrigerated vehicle. Constraint (8) ensures that the total fresh product transportation volume among FDCs does not exceed the capacity of a single refrigerated truck. Constraint (9) ensures that the amount of fresh product transported is equal to the total reassigned customer demands among FDCs. Constraints (10)–(11) ensure the continuity of the delivery process and that the unloading service time is excluded. Constraints (12)–(13) express the arrival time of a refrigerated vehicle departing from the FDC and arriving at the customers. Constraints (14)–(15) express arrive time of a refrigerated truck at the FDCs. Constraint (16) eliminates sub-tours on a distribution route. Constraint (17) ensures that each customer is served by only one refrigerated vehicle. Constraint (18) ensures that each refrigerated vehicle serves only one distribution route within the  $\pi$ th service time period. Constraint (19) stipulates that a refrigerated vehicle must leave each customer after serving the customer within the  $\pi$ th service time period. Constraints (20)–(21) indicate that each customer is visited once. Constraint (22) ensures that the departure time of each refrigerated vehicle is within the time window of the FDC. Constraint (23) guarantees that the total travel time of a refrigerated vehicle does not exceed the maximum allowed en-route time. Constraints (24)–(31) state the binary decision variables.

### 3.3. Coefficient of performances at different temperatures

In cold chain transportation, the in-vehicle temperature determines the TCC and the product VL. Given that different types of fresh products have different temperature control ranges, the refrigerated vehicles should be set to suitable refrigerating temperatures according to the characteristics of the fresh products. Considering the characteristics of heat change, the coefficient of performance (COP) (Song, et al., 2019) in Eq. (32) represents the conversion ratio between energy and heat.

$$COP = \frac{Q}{W^+} = \frac{T_b}{T_a - T_b} \tag{32}$$

In Eq. (32),  $Q$  refers to the heat required to transition from low temperature to high temperature,  $W^+$  represents the absorbed energy,  $T_a$  is the temperature of the ambient environment (e.g., 25 °C), and  $T_b$  represents the target temperature for temperature control (e.g., 5 °C).  $T_a$  and  $T_b$  must be calculated as absolute temperatures. The physical quantity corresponding to the absolute temperature is the thermodynamic temperature, represented as  $T(K)$ . The corresponding unit is Kelvin (Vřešťál, et al., 2012) and the symbol is  $K$ . The relationship between thermodynamic temperature  $T(K)$  and Celsius temperature  $t(°C)$  is shown in Eq. (33).

$$T(K) = 273 + t(°C) \tag{33}$$

If the external ambient temperature is 25 °C, then the cooling cost at the control target temperature of 5 °C is 1 unit, and the cooling cost

**Table 4**  
Corresponding relationships between  $w$  and temperature.

$w$ of Set $W$	1	2	3	4	5	6	7	...	18	...	27
Temperature ( $^{\circ}\text{C}$ )	5	4	3	2	1	0	-1	...	-12	...	-21

**Table 5**  
COP values,  $g_{mw}$ ,  $\theta_{mw}$  of different temperature intervals.

Temperature ( $^{\circ}\text{C}$ )	5	4	3	2	1	0	-1	-2	-3
COP	13.90	13.19	12.55	11.96	11.42	10.92	10.46	10.04	9.64
$\theta_{mw}$	1.00	1.05	1.11	1.16	1.22	1.27	1.33	1.38	1.44
$g_{mw}$	2.00	2.11	2.22	2.33	2.44	2.55	2.66	2.77	2.88
Temperature ( $^{\circ}\text{C}$ )	-4	-5	-6	-7	-8	-9	-10	-11	-12
COP	9.28	8.93	8.61	8.31	8.03	7.76	7.51	7.28	7.05
$\theta_{mw}$	1.50	1.56	1.61	1.67	1.73	1.79	1.85	1.91	1.97
$g_{mw}$	3.00	3.11	3.22	3.34	3.46	3.58	3.70	3.82	3.94
Temperature ( $^{\circ}\text{C}$ )	-13	-14	-15	-16	-17	-18	-19	-20	-21
COP	6.84	6.64	6.45	6.27	6.10	5.93	5.77	5.62	5.48
$\theta_{mw}$	2.03	2.09	2.16	2.22	2.28	2.34	2.28	2.47	2.54
$g_{mw}$	4.06	4.18	4.31	4.44	4.56	4.69	4.57	4.94	

coefficient ( $\theta_{mw}$ ) at 4  $^{\circ}\text{C}$  is  $13.9/13.19 = 1.05$ , as shown in Table 5. The same method can be used to calculate the cooling cost coefficient under other temperature control conditions. In addition, the unit temperature control cost ( $g_{mw}$ ) at different temperature control conditions can be calculated using Eq. (34). We assume 27 temperature control ranges for  $w$ , and the corresponding control target is shown in Table 4. The corresponding COP values and unit temperature control costs at different control target temperatures are shown in Table 5.

$$g_{mw} = \begin{cases} \sigma_c \cdot f_{kw} \cdot \theta_{mw}, & \text{if transported by refrigerated truck } k \\ \sigma_q \cdot f_{vw} \cdot \theta_{mw}, & \text{if transported by refrigerated vehicle } v \end{cases} \quad (34)$$

#### 4. Research methodologies

##### 4.1. Hybrid heuristic algorithm for the CMCVRP-RSTC optimization

The proposed CMCVRP-RSTC is essentially a multi-objective optimization problem, and the NSGA-II is a well-known evolutionary algorithm for solving this type of problem (Deb et al., 2002). The NSGA-II has the advantages of fast computation and can find the global optimum. Meanwhile, the tabu search (TS) algorithm focuses on neighborhood search and finding the local optimum (Zhan et al., 2013; Su et al., 2017). We propose a TS-NSGA-II hybrid algorithm that combines k-means clustering, TS, and NSGA-II to effectively solve the CMCVRP-RSTC. The framework of the hybrid algorithm for solving the CMCVRP-RSTC is shown in Fig. 3. The parameters used in the algorithm are defined as follows:  $h$  and  $q$  are the numbers of FDCs and clustering units, respectively;  $gen_{max}$  is the maximum number of generations in the NSGA-II algorithm;  $tsin$  is the maximum number of iterations in the TS algorithm; and  $gen$  and  $t$  denote the current generation and iteration, respectively.

##### 4.1.1. Customer clustering

Customer clustering can effectively reduce the computational complexity of large-scale logistics network optimization problems by assigning customers to groups and treating customers in a group the same (Wang et al., 2017b; Markova et al., 2016). The extended k-means clustering algorithm is applied to customer clustering. The clustering features include each customer's geographical coordinates, the temperature control characteristics of the customer's demands, and the service time windows.

In this paper, modified Manhattan distance is adopted as the distance function for clustering. The coordinates, the TCR, and the service time windows of customers are denoted as  $(x, y)$ ,  $(tp, cp)$ , and  $(st, tm)$ , respectively. The modified Manhattan distance between customers  $i$  and

$j$  is evaluated as  $d_{ij} = |x_i - x_j| + |y_i - y_j| + \tilde{U} * |tp_i - tp_j| + \tilde{U} * |cp_i - cp_j| + \tilde{\epsilon} * |st_i - st_j| + \tilde{\epsilon} * |tm_i - tm_j|$ , and coefficients  $\tilde{U}$  and  $\tilde{\epsilon}$  ensure that the different dimensions are at the same scale. The 4D clustering framework is displayed in Fig. 4.

In Fig. 4, the geographic location and the time window are represented as X, Y-axes, and the time-axis respectively. That is, customers can be first clustered based on the temperature range  $[t_1, t_2]$  and the time window  $[a_5, a_4]$ . Then the space range can be considered to cluster the above customers. The clustering algorithm is executed when the CMFLDN has at least two FDCs. The extended k-means clustering algorithm is shown in Table 6 as follows.

##### 4.1.2. TS-NSGA-II

In the NSGA-II framework, fast non-dominated sorting is applied to find a good set of solutions that nearest the Pareto optimal front, the crowding distance is calculated to retain the diversity of the Pareto optimal solutions, and the elitism strategy is introduced to improve the convergence of solutions (Arora et al., 2015; Alikar et al., 2017). We propose an optimization method based on the combination of the NSGA-II framework with the local search by the TS algorithm. The TS strategy is documented and selected during the optimization process, and a flexible storage structure and the corresponding tabu criterion are presented to avoid a roundabout search (Martínez-Puras & Pacheco, 2016, Silvestrin & Ritt, 2017; Li et al., 2019). The TS-NSGA-II hybrid algorithm explores the solution space both locally and globally to ultimately achieve global optimization. Routes are first organized globally through NSGA-II, and then adjusted locally by local search using TS, as shown in Fig. 5.

The TS-NSGA-II hybrid algorithm is based on the result of extended k-means customer clustering. This algorithm follows the principle of "survival of the fittest" and has the advantages of strong search ability, parallel comparison and strong scalability. The pseudo code of the proposed TS-NSGA-II algorithm is shown in Table 7.

##### 1. Genetic manipulation process

Considering the encoding method used, the refrigerated vehicles can simultaneously perform resource sharing and temperature control. Partial mapped crossover (PMC) is employed to generate an offspring population (Wang et al., 2019a), by exchanging the partial strings of two selected parents (Pa). The intermediate sequence is set to an independent chromosome, PMC is selected as a crossover operator, which means that the subsequence of each chromosome acts as a crossover region, and then, two crossover regions are exchanged to obtain two new offspring chromosomes (Ch). The crossover operation is illustrated in Fig. 6.

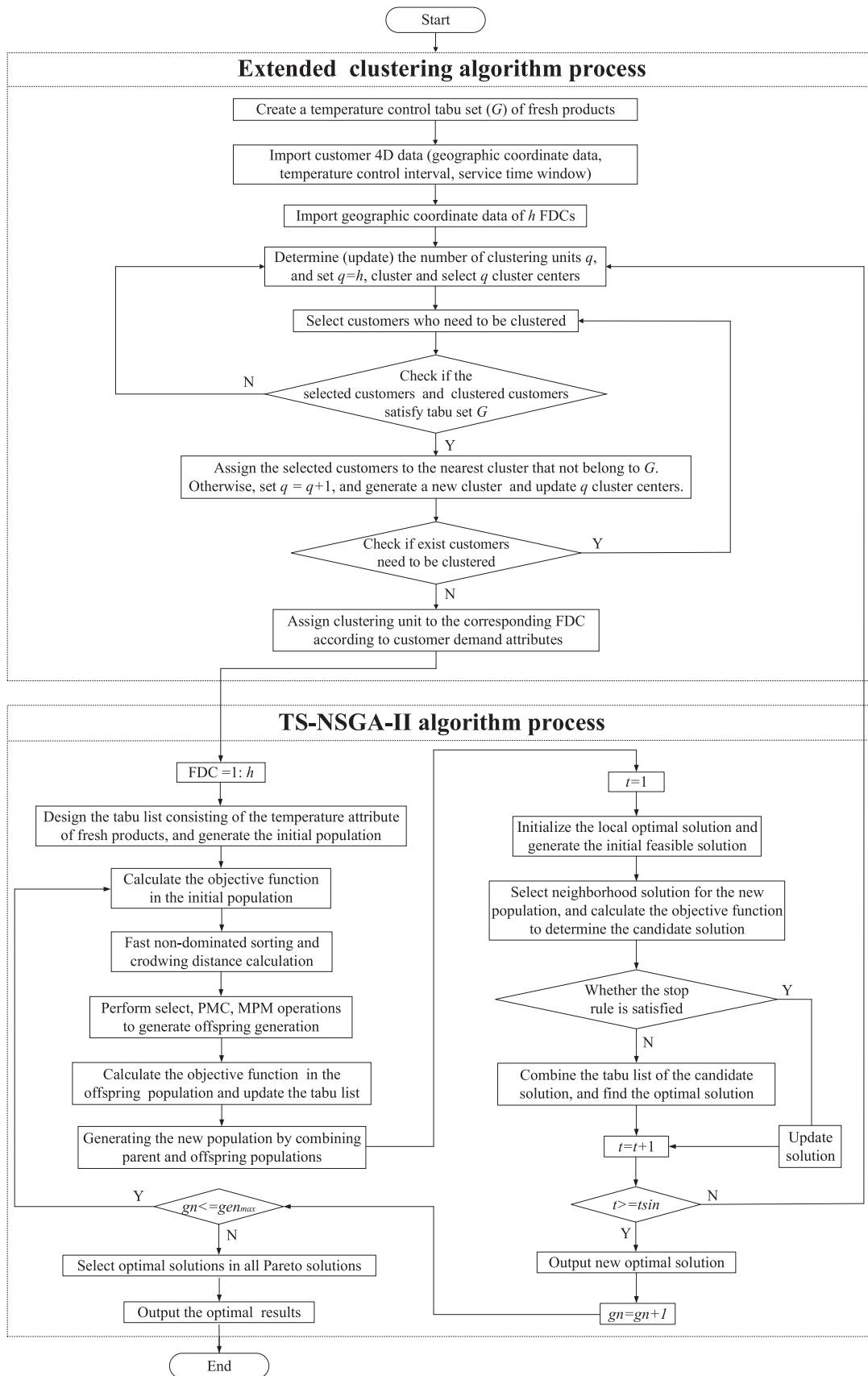


Fig. 3. Algorithm flowchart of CMCVRP-RSTC.

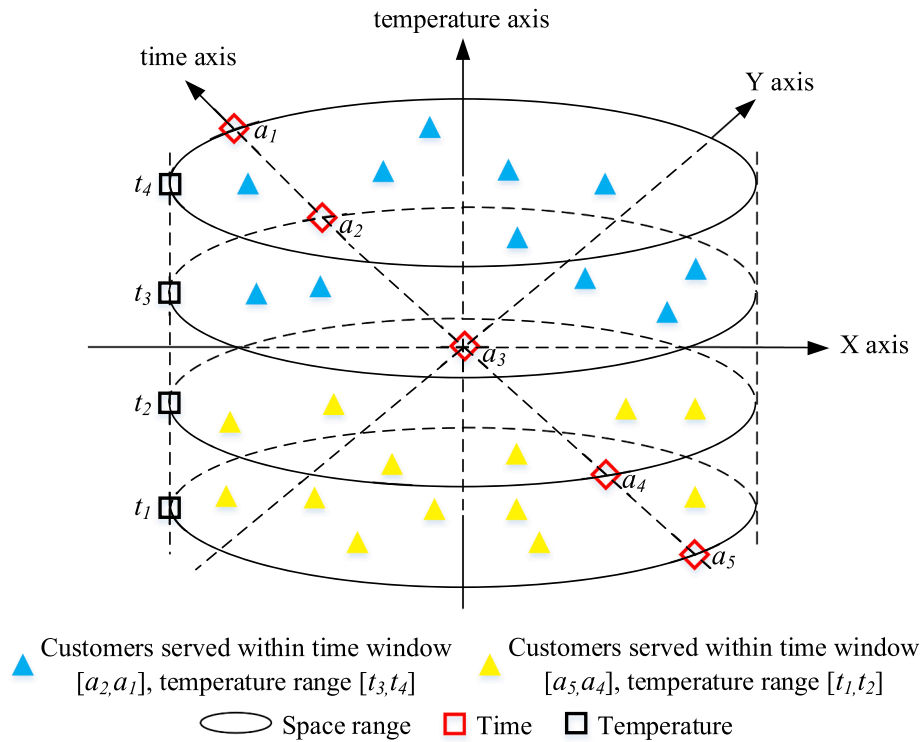


Fig. 4. Extended k-means customer clustering diagram.

Table 6

Procedure of extended k-means clustering algorithm.

<i>Arithm 1: Extended k-means clustering</i>
<b>Step 1:</b> Create the temperature control TS $G$ of fresh products, and select customers whose product demand attributes cannot satisfy $G$ .
<b>Step 2:</b> Import the customer's corresponding 4D data and the geographic coordinates of $h$ FDCs to generate a data matrix.
<b>Step 3:</b> Convert the 4D data matrix into data vector.
<b>Step 4:</b> Determine initial clustering number $q$ , and set $q = h$ ; then, cluster and select $q$ cluster centers.
<b>Step 5:</b> Select the customers who must be clustered by the customer product demand data.
<b>Step 6:</b> Check if the selected and clustered customers satisfy TS $G$ in each clustering unit.
<i>If <math>G</math> is satisfied, then the selected customers are assigned to the nearest clustering unit that not satisfy <math>G</math>. Otherwise, set <math>q = q + 1</math>, generate new clustering units, and update the clustering center. Else, return to Step 4. EndStep 7:</i> Determine if the existing customers must be clustered. <i>If existing customers must be clustered, repeat Steps 5–7 until the cluster relationship is constant. Else, assign the clustering unit to the corresponding FDC according to the customer product demand attributes.</i>
<b>End</b>
<b>End</b>

The chromosomes in the initial parent population are encoded as Pa1 and Pa2 in Fig. 6. If  $i$  is the total number of customers served by a FDC, then  $i + 1$  is added into the initial string to express customer quantity. The fresh products required by customers can be divided into different products types (i.e., a, b, and c) under the same temperature control range (e.g., a kind of temperature control range “(1 °C)–(5 °C)”) through clustering. Two points (A and B) are selected on chromosomes Pa1 and Pa2. Then, the sequence between A and B is set as an independent chromosome, and PMX operation is carried out. The child chromosome (Ch) is generated, namely, multi-point mutation (MPM) is implemented on the parent chromosome (Pa), and the mutation operator is conducted with a small probability. Fig. 7 illustrates an illustration of the mutation operator.

In Fig. 7, the fresh products required by customers are divided into different types (i.e., a and b) of products under the same TCR (e.g., a kind of temperature control range “(-5 °C)–(0 °C)”). First, four nodes (i.e., 5, 7, 2, 9) are randomly selected in the Pa. Then, MPM is performed on the four nodes to generate Ch. For the blue nodes, if the value of the gene does not exceed 6, then the gene is the same as the original gene (e.g., 5 remains unchanged in Ch). Moreover, for the orange nodes, if the value of the gene exceeds 6, then the value of the gene is randomly

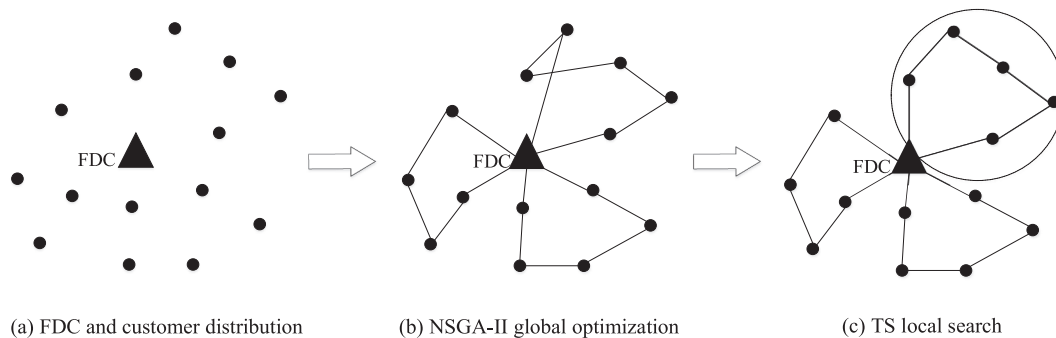


Fig. 5. General diagram of algorithm optimization.

**Table 7**  
Procedure of TS-NSGA-II.

*Arithm 2: TS-NSGA-II*

**Step 1:** Initialize the corresponding parameters, generate the initial population, and set the tabu list containing the temperature control of fresh products. # Set the appropriate population size ( $pop_{size}$ ), the maximum number of generations ( $gen_{max}$ ), and the maximum number of iterations ( $tsin$ ) in TS.

# Set the genetic parameters: selection probability  $P_s$ , crossover probability  $P_c$ , and mutation probability  $P_m$ .

for  $FDC = 1: h$  **Step 2:** Calculate the objective function value of each chromosome in the initial population.

# **Step 3:** Conduct fast non-dominated sorting and calculation of crowding distance in the population.

# **Step 4:** Perform selection, partial mapped crossover (PMC), and multi-point mutation (MPM) operations to generate the offspring population.

**Step 5:** Evaluate the objective value of each chromosome in the offspring population, and update the tabu list.

**Step 6:** Combine the parent and offspring populations to generate a new population and ensure that the current best chromosomes are added to the population.

**Step 7:** Apply the TS strategy to the initial solution based on NSGA-II and set  $t = 1$ .  
(7.1) Initialize the NSGA-II optimization solution and define the neighborhood movement to obtain the neighbor solution of the TS new population. (7.2) Calculate the objective function value of each chromosome in the current new population, perform new population neighborhood selection, and record the optimal solution to determine the candidate solution. (7.3) Determine whether the TS stop rule is satisfied. If the TS stop rule is satisfied, then update the current optimal solution, use it as the initial solution for the next iteration, and execute  $t = t + 1$ . Else, perform (7.4). (7.4) Combine the tabu attribute of the candidate solution, find the optimal solution from the current candidate solution, use it as the initial solution for the next iteration, and execute  $t = t + 1$ . (7.5) Determine if  $t$  is greater than or equal to  $tsin$ . If  $t$  is greater than or equal to  $tsin$ ,  $gn = gn + 1$  is executed according to the new optimized solution generated by the TS strategy. Else, perform **Step 4** in the clustering process. **EndStep 8:** Determine if the number of iterations  $gn$  is less than or equal to the maximum number of iterations ( $gen_{max}$ ). If  $gn$  is less than or equal to  $gen_{max}$ , return to **Step 2**. Else, perform **Step 9**. **Step 9:** Find the optimal solution in all Pareto fronts and output the final optimization solution.

End

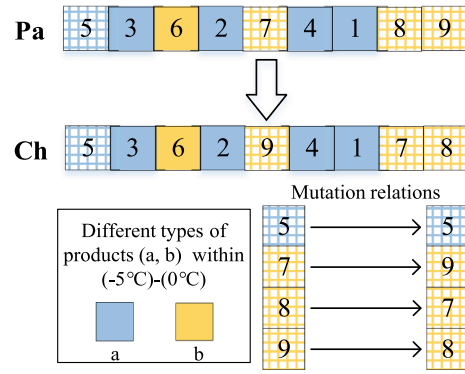


**Fig. 7.** Multi-Point Mutation operator.

**Table 8**  
Related notations in profit allocation.

$C_0(n)$	Cost for player $n$ without coalition
$C(S)$	Total cost in coalition $S$
$v^+(S)$	Profit in coalitions $S$
$\chi$	Coordination requirement of LSP
$\Lambda$	Set of possible sequences of forming the grand coalition $N$
$\varphi(N, v^+)$	MCRS value allocated to a certain player in the coalitions
$\omega(n)$	Rank of player
$\eta(n, \omega, u)$	Cost reduction percentages to player $n$ on step $u$ in sequence $\omega$

achieve significant cost savings by joining a coalition. The LSP will retain a certain percentage of the total profit as a charge for organizing the collaboration, before distributing the rest of the profit to each participant. The retained percentage is called the coordination requirement and defined as  $\chi \in [0,1]$ . The cost savings and the LSP's income can be calculated according to Eq. (35). The LSP receives this profit as  $P_{LSP}$ , and fresh logistics facilities share  $v^+(S)$  according to Eq. (36).

$$P_{LSP} = \chi \cdot \sum_{n \in S} C_0(n) - C(S) \quad (35)$$

$$v^+(S) = \begin{cases} (1 - \chi) \cdot \sum_{n \in S} C_0(n) - C(S), & \text{if } \sum_{n \in S} C_0(n) - C(S) \geq 0 \\ 0, & \text{otherwise} \end{cases} \quad (36)$$

The corresponding cost savings for each coalition ( $v^+(S)$ ) is calculated as the gap between initial cost  $C_0(n)$  and optimization cost  $C(S)$ . If  $\sum_{n \in S} C_0(n) - C(S) < 0$ , then alliance  $S$  will not be formed, resulting in zero profit.

The MCRS is a quadratic assignment method of achieving fair cost or profit allocation in alliance problems (Tijs & Driessen, 1986; Wang et al., 2017a, 2018). This method is bi-level. The method first allocates a portion of the profit directly and then distributes the residual profit. We set  $N$  as the set of all participants, and  $N = \{1, 2, \dots, n\}$ . First, the upper bound ( $y_{nmax}$ ) and the lower bound ( $y_{nmin}$ ) of profit  $y_n$  are determined. Then, distribution vectors  $Y_{min}$  and  $Y_{max}$  can be respectively expressed as  $Y_{min} = \{y_{1min}, y_{2min}, \dots, y_{nmin}\}$  and  $Y_{max} = \{y_{1max}, y_{2max}, \dots, y_{nmax}\}$ . The upper and lower bounds are related by Eq. (37). Coefficient  $\lambda$  in Eqs. (37) and (38) is determined by the ratio of the difference between the maximum and minimum benefits for member  $n$  to the sum of all member income differences. The limits of distribution vector  $Y$  can be derived using Eq. (39).

$$Y = Y_{min} + \lambda \sum_{n \in N} y_{nmax} - \sum_{n \in N} y_{nmin} \quad (37)$$

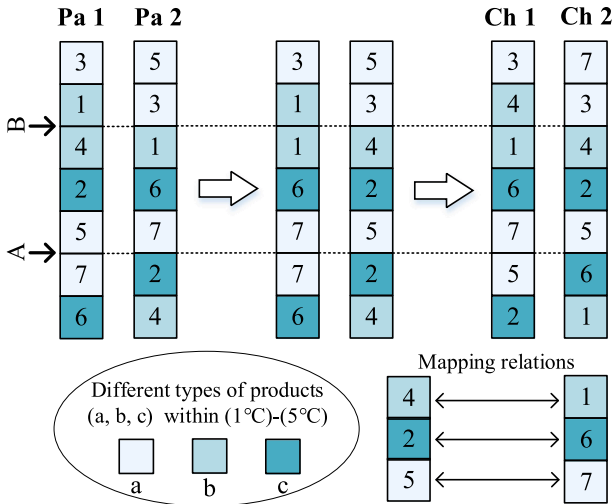


**Fig. 6.** Partial Mapped Crossover process.

regenerated from 7. To avoid duplication with existing genes, 7 can be changed to 9, 8 can be changed to 7, and 9 can be changed to 8.

**4.2. Profit allocation and coalition stability evaluation**

Let  $N$  be a set of FDCs, then  $2^N - 1$  subsets of  $N$  exist, excluding the null set (Wang et al., 2017b). Let  $S$  be one of the  $2^N - 1$  subsets, that is, a coalition. The notations related to profit allocation are listed in Table 8.

**4.2.1. Cost savings calculation and MCRS model**

Through CMCVRP-RSTC optimization, each FDC has the potential to

$$\lambda = \frac{y_{nmax} - y_{nmin}}{\sum_{n \in N} y_{nmax} - \sum_{n \in N} y_{nmin}} \quad (38)$$

$$Y_{min} \leq Y \leq Y_{max} \quad (39)$$

Furthermore, the hyper-plane is determined by Eq. (40), and the profit allocation by MCRCs value  $\varphi(N, v^+)$  can be expressed as Eq. (41).

$$\sum_{n \in N} y_n = v^+(N) \quad (40)$$

$$\varphi_n(N, v^+) = y_{nmin} + \frac{y_{nmax} - y_{nmin}}{\sum_{n \in N} (y_{nmax} - y_{nmin})} \times v^+(N) - \sum_{n \in N} y_{nmin} \quad (41)$$

We can respectively calculate  $y_{nmax}$  and  $y_{nmin}$  through the following linear programming Eqs. (42) and (43).  $v^+(S)$  is the cost reduction for the players who participate in collaborative alliance  $S$ , and  $S \subseteq N$ .  $v^+(N)$  denotes the total cost reduction after forming a grand coalition that consists of all customers and FDCs. Eqs. (44) and (45) set the bounds of the profit of each coalition and that of each participant.

$$y_{nmax} = v^+(S) - v^+(S - \{n\}) \quad (42)$$

$$y_{nmin} = v^+(n) \quad (43)$$

Subject to

$$y_n \geq v^+(n) \quad (44)$$

$$\sum_{n \in S} y_n \geq v^+(S) \quad (45)$$

#### 4.2.2. Monotonic path selection strategy

Grand coalition  $N$  is formed with multiple different sequences, and the profit assigned to participants varies with each sequence. The best sequence of entry into the coalition is determined according to the monotonic path selection rules (Crujssens et al., 2007). Set  $\omega$  as one of these sequences and let  $\omega(n)$  indicate that player  $n$  joins  $\omega$  as the  $\omega(n)$ 'th member. The cost saving percentage for player  $n$  in sequence  $\omega$  when the  $u$ th player joins the coalition is denoted as  $\eta(n, \omega, u)$ , which can be calculated using Eq. (46).

$$\eta(n, \omega, u) = \frac{\varphi_n(\cup_{\omega(u) \leq u, \mu \in N} H, v)}{C_0(n)}, u \geq \omega(n) \quad (46)$$

If  $\Lambda$  is the set of sequences to form grand coalition  $N$ , then  $\Lambda$  has  $|N|!$  different sequences. Coalition sequences that follow the strictly monotonic path (SMP) rule are considered stables (Lozano et al., 2013; Wang et al., 2017b). An optimal coalition sequence is stable and allocates the total profit fairly among coalition members.

All profit allocation schemes can be represented as a polygon, with each of its boundary indicating a profit allocation scheme. The geometric center of this polygon (called the "core center") is theoretically the fairest profit allocation scheme among all schemes. Eq. (47) is used to calculate the position of the core center, where  $\alpha$  is a parameter for controlling the scope of the core.

$$\frac{v^+(N) - v^+(N - \{n\})}{v^+(N)} \times \alpha + \sum_{c \in N}^{c \neq n} y_c = v^+(N - \{n\}) \quad (47)$$

### 5. Implementation and analysis

#### 5.1. Algorithms comparison

To test the performance of the proposed TS-NSGA-II, comparisons with well-known heuristic algorithms are made on solving benchmark problems. The proposed TS-NSGA-II algorithm, multi-objective particle swarm optimization (MOPSO) (He et al., 2019), and hybrid genetic algorithm-tabu search (HGA-TS) (Xiao et al., 2018) are implemented with 20 selected experimental data instances for comparison based on

**Table 9**  
Characteristics of the datasets.

Data instances	No. of customers	No. of FDCs	Temperature control range	Product type	Product price
1-4	80	8,6,4,2	(-5 °C)-(0 °C) (1 °C)-(5 °C)	Cc1 Dd1	6 4
5-8	100	8,6,4,2	(-5 °C)-(0 °C) (-13 °C)-(-8 °C)	Cc1 Bb1	6 9
9-12	120	9,7,5,3	(-5 °C)-(0 °C) (1 °C)-(5 °C) (-13 °C)-(-8 °C)	Cc1 Dd1 Bb1	6 4 9
13-16	150	9,7,5,3	(-5 °C)-(0 °C) (-13 °C)-(-8 °C) (1 °C)-(5 °C) (-20 °C)-(-15 °C)	Cc1 Bb1 Dd1 Aa1	6 9 4 11
17-20	180	10,8,6,4	(-5 °C)-(0 °C) (-13 °C)-(-8 °C) (1 °C)-(5 °C) (-20 °C)-(-15 °C)	Cc1 Bb1 Dd1 Aa1	6 9 4 11

the Solomon datasets (Solomon, 1987) and the MDVRPTW instances<sup>1</sup>. All customer product demands are assigned into 2-4 temperature control ranges. For example, in Data instances 1-4, the temperature control range of the first 40 customers is (-5°C)-(0°C), and the temperature control range of the last 40 customers is (1°C)-(5°C). Each temperature control range has one type of fresh products and one corresponding product price. The experimental data instances are described in Table 9.

The parameters utilized in the comparison of the algorithm performance are set as follows:  $pop_{size} = 150$ ,  $gen_{max} = 500$ ,  $P_s = 0.9$ ,  $P_c = 0.8$ ,  $P_m = 0.1$ ,  $tsin = 50$  in TS-NSGA-II and HGA-TS. The swarm size  $pop_{size} = 150$ , inertia weight  $it_w = 0.5$ , maximum number of iterations  $it_{max} = 500$  in MOPSO. The optimization results have four aspects, that is, the total cost, the VL, the minimal number of refrigerated vehicles, and the computation time of three algorithms are compared. The three algorithms are executed 10 times with the known optimal solutions for the 20 data instances selected, and the comparison of results is shown in Table 10.

The optimization results show that TS-NSGA-II exhibits the best performance in most of the 20 data instances. In the same instance, TS-NSGA-II always returns the smallest cost and VL among the three algorithms and outperforms or ties with the other two algorithms in minimizing the number of vehicles. However, the computation of TS-NSGA-II is slower than that of HGA-TS. On the average, our proposed TS-NSGA-II approach produces significantly ( $p$ -value < 0.05) better optimization results at the price of higher computation time than HGA-TS. Considering that optimizing fresh logistics networks involves long-term decisions and thus has low real-time requirement, the proposed TS-NSGA-II has clear advantages over the other two algorithms in practical applications.

#### 5.2. Data source

The applicability and feasibility of the proposed CMCVRP-RSTC is studied in the context of the real logistics network of Chongqing City. Chongqing City is located in Southwestern China and serves as a national transportation hub and a trade center in the upper Yangtze River. Consequently, the logistics network in the city is complex. The logistics network consists of five FDCs (i.e., FDC1, FDC2, FDC3, FDC4, FDC5) and

<sup>1</sup> <http://neo.lcc.uma.es/vrp/vrp-instances/multiple-depot-vrp-with-time-windows-instances/>

**Table 10**  
Comparison of algorithm performance.

Instance	TS-NSGA-II				MOPSO				HGA-TS			
	Cost	Loss of value	No. of vehicles	Time (s)	Cost	Loss of value	No. of vehicles	Time (s)	Cost	Loss of value	No. of vehicles	Time (s)
1	2013	389	13	172	1979	409	13	175	2223	462	15	167
2	1971	395	12	164	2002	421	13	162	2336	477	14	160
3	1995	392	12	160	2068	433	12	160	2385	481	13	156
4	2140	408	12	156	2152	445	12	153	2416	495	12	149
5	2252	469	16	182	2491	489	17	185	2563	533	18	178
6	2281	485	15	176	2514	502	16	182	2653	551	17	167
7	2305	490	15	178	2493	496	15	177	2679	560	16	161
8	2395	504	14	171	2579	524	15	165	2721	579	14	154
9	2588	577	18	192	2616	595	18	193	2853	640	20	185
10	2694	590	18	186	2632	597	18	189	2915	651	19	181
11	2612	581	17	190	2701	617	17	191	2950	679	18	176
12	2761	627	16	175	2852	658	16	172	3042	702	17	163
13	3011	651	22	202	3356	692	23	203	3352	794	23	195
14	3029	664	21	192	3299	681	22	201	3389	813	22	187
15	3135	676	22	180	3495	704	21	182	3442	829	21	179
16	3197	682	20	170	3508	726	20	173	3511	864	20	174
17	3578	711	26	219	3715	792	27	220	3965	901	28	209
18	3599	723	25	203	3827	845	26	208	4062	939	26	201
19	3653	736	26	199	3899	861	26	201	4114	976	26	189
20	3710	752	25	190	4009	925	25	193	4130	981	25	178
Average	2746	575	18	183	2909	621	19	184	3085	695	19	175
t-test	-5.98	-4.77	-	-1.94	-23.02	-9.17	-	6.53	-	-	-	-
p-value	3.8E-06	5.8E-05	-	3.3E-02	3.6E-16	6.6E-09	-	1.1E-06	-	-	-	-

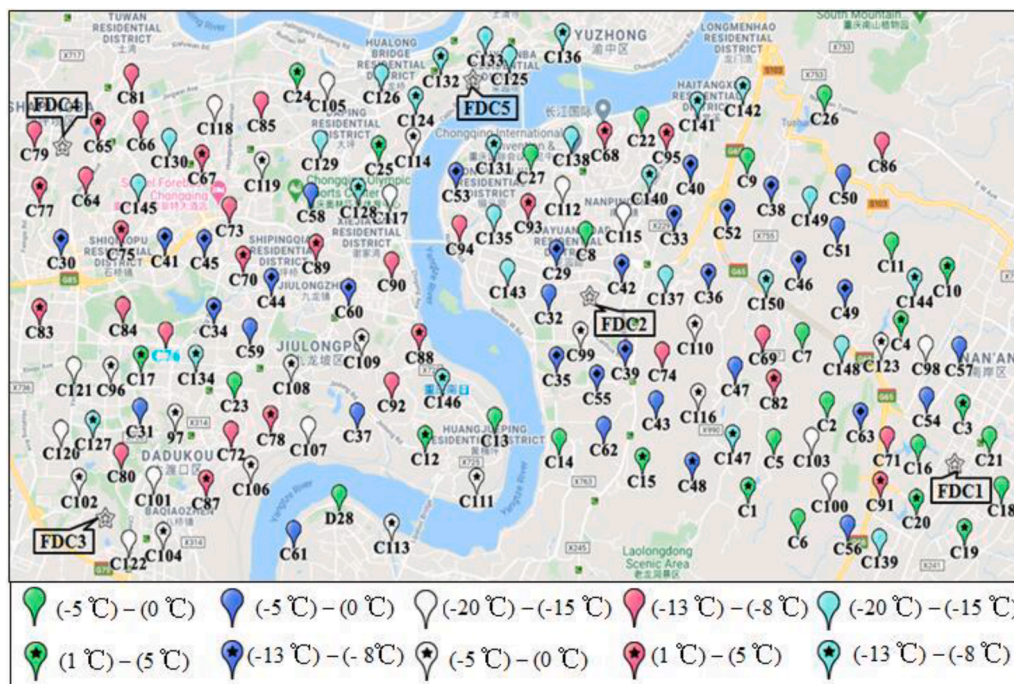


**Fig. 8.** Geographical distribution of customers and FDCs.

**Table 11**  
Different product types under the four temperature control ranges.

Temperature control range	(-20 °C)-(-15 °C)	(-13 °C)-(-8 °C)	(-5 °C)-(0 °C)	(1 °C)-(5 °C)
Fresh product type	Aa1, Aa2	Bb1, Bb2, Bb3	Cc1, Cc2, Cc3	Dd1, Dd2

150 representative customers (i.e., C1, C2, ..., C150) as illustrated in Fig. 8. Ten types of fresh products are distributed in four temperature control ranges. Each temperature control range has 2-3 types of fresh products. The correspondence of each type of fresh products with the temperature control range is given in Table 11. For example, fresh product types Aa1 and Aa2 require a temperature control range of (-20 °C)-(-15 °C).

The initial customer assignment to each FDC and the temperature control ranges required by each FDC are shown in Table 12. Additional information includes customer service time windows, customer demands, fresh product prices, temperature control ranges, fresh product

**Table 12**  
Correspondence among facilities, customers, and temperature control ranges.

Facility	FDC1	FDC2	FDC3	FDC4	FDC5
Customer	C1C2C3C4C5C 6C7C8C9C10C1 1C12C13C14C15C1 6C17C18C19C20C2 1C22C23C24C25C26C27C28	C29C30C31C32 C33C34C35C36C 37C38C39C40C4 1C42C43C44C45C4 6C47C48C49C50C51 C52C53C54C55C56C 57C58C59C60 C61C62C63	C96C97C98C99C 100C101C102C103C 104C105C106C107C108C 109C110C111C112 C113C114C115C116C117 C118C119C120C121C122C123	C64C65C66C67C68C69C70C71 C72C73C74C75C76C77C78C79 C80C81C82C83C84C85C86C87 C88C89C90C91C92C93C94C95	C124C125C126C127C128C129 C130C131C132C133C134C135 C136C137C138C139C140C141 C142C143C144C145C146C147 C148C149C150
Temperature control range	(-5 °C)-(0 °C) (1 °C)-(5 °C)	(-5 °C)-(0 °C) (-13 °C)-(-8 °C)	(-20 °C)-(-15 °C) (-5 °C)-(0 °C)	(-13 °C)-(-8 °C) (1 °C)-(5 °C)	(-20 °C)-(-15 °C) (-13 °C)-(-8 °C)

types, and FDCs' service time windows, which can be found in [Tables A1 and A2](#) in [Appendix A](#). Prior to optimization, the service coverage areas of the FDCs intersect with each other. Customers are assigned to FDCs without considering their geographical locations, increasing the loss of value of perished fresh products, transportation costs, and thus the total logistics operational costs. Therefore, effective collaborative mechanism and rational resource configuration are studied in this case to optimize vehicle routing/scheduling and the temperature control ranges of fresh products by solving the CMCVRP-RSTC.

5.3. Parameter setting and optimization results

The goal of CMFLDN optimization is to find the routing solution with the lowest total cost and number of refrigerated vehicles. The parameter values in the optimization model and the TS-NSGA-II initialization are determined based on existing research ([Govindan et al., 2014](#); [Wang et al., 2015](#)) and are set as follows:  $\sigma_q = 4.4$ ,  $\sigma_c = 3.4$ ,  $f_{vw} = 3.2$ ,  $f_{kw} = 6.6$ ,  $Q_v = 1800$ ,  $Q_k = 200$ . When persuading FDCs to collaborate, the following incentives offered by the LSP:  $\gamma_1 = 0.1$ ;  $\gamma_2 = 0.09$ ;  $\gamma_3 = 0.1$ ;

**Table 13**  
Comparison between initial and optimized networks for each coalition scenario.

Coalitions	Initial network			Optimized network		
	Total cost	No. of vehicles	Value loss	Total cost	No. of vehicles	Value loss
{DC1}	1019	5	172	917	5	164
{DC2}	891	6	141	811	6	133
{DC3}	1175	5	191	1058	5	183
{DC4}	1098	5	180	999	5	175
{DC5}	979	4	149	871	4	140
{DC1, DC4}	2117	10	352	1542	9	198
{DC1, DC5}	1998	9	321	1388	9	173
{DC2, DC4}	1989	11	321	1554	10	191
{DC2, DC5}	1870	10	290	1325	9	169
{DC3, DC4}	2273	10	371	1736	10	190
{DC3, DC5}	2154	9	340	1567	9	175
{DC1, DC2}	1910	11	313	1342	9	166
{DC1, DC3}	2194	10	363	1783	9	199
{DC2, DC3}	2066	11	332	1552	9	164
{DC4, DC5}	2077	9	329	1624	9	170
{DC1, DC2, DC4}	3008	16	493	2268	15	255
{DC1, DC2, DC5}	2889	15	462	2128	13	244
{DC1, DC3, DC4}	3292	15	543	2281	14	258
{DC1, DC3, DC5}	3173	14	512	2360	14	252
{DC2, DC3, DC4}	3164	14	517	2312	15	243
{DC2, DC3, DC5}	3045	15	481	2260	13	237
{DC1, DC4, DC5}	3096	14	501	2118	13	251
{DC2, DC4, DC5}	2968	15	470	2148	14	246
{DC3, DC4, DC5}	3252	14	520	2083	13	254
{DC1, DC2, DC3}	3085	16	504	2171	15	257
{DC1, DC2, DC4, DC5}	3987	20	642	2570	18	283
{DC1, DC3, DC4, DC5}	4271	19	692	2735	18	305
{DC2, DC3, DC4, DC5}	4143	20	661	2650	18	290
{DC1, DC2, DC3, DC4}	4183	21	684	2827	19	311
{DC1, DC2, DC3, DC5}	4064	20	653	2685	17	302
{DC1, DC2, DC3, DC4, DC5}	5162	25	833	3030	23	363

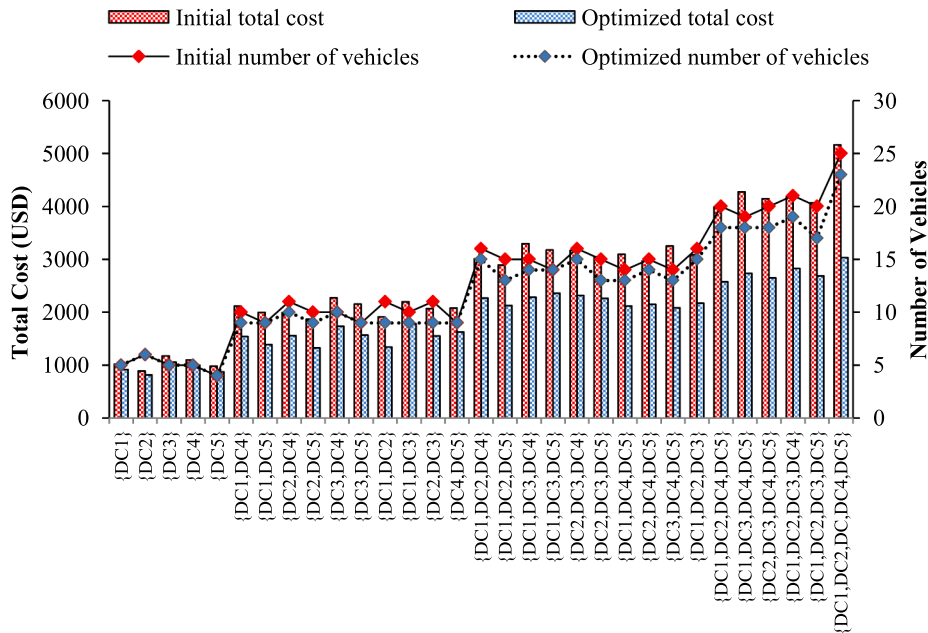


Fig. 9. Comparison between initial and optimized cost and number of vehicles.

Table 14

Decomposed costs for DC1, DC2, DC3, DC4 and DC5 in the grand coalition after CMFLDN optimization.

Facility	TC2 and TC4 of all fresh product types										TC <sub>1</sub>	TC <sub>3</sub>	TLOC (\$)		
	Cc1 (\$)		Cc2 (\$)		Cc3 (\$)		Dd1 (\$)		Dd2 (\$)						
DC1	TC <sub>2</sub>	TC <sub>4</sub>	TC <sub>2</sub>	TC <sub>4</sub>	TC <sub>2</sub>	TC <sub>4</sub>	TC <sub>2</sub>	TC <sub>4</sub>	TC <sub>2</sub>	TC <sub>4</sub>	202	71	486		
	31	10	28	13	34	16	27	10	29	15					
DC2	Bb1 (\$)		Bb2 (\$)		Bb3 (\$)		Cc1 (\$)		Cc2 (\$)		Cc3 (\$)		388	153	807
	TC <sub>2</sub>	TC <sub>4</sub>	TC <sub>2</sub>	TC <sub>4</sub>	TC <sub>2</sub>	TC <sub>4</sub>	TC <sub>2</sub>	TC <sub>4</sub>	TC <sub>2</sub>	TC <sub>4</sub>	TC <sub>2</sub>	TC <sub>4</sub>			
	41	21	29	14	20	12	34	19	25	11	26	14			
DC3	Aa1 (\$)		Aa2 (\$)		Cc1 (\$)		Cc2 (\$)		Cc3 (\$)		258	122	635		
	TC <sub>2</sub>	TC <sub>4</sub>	TC <sub>2</sub>	TC <sub>4</sub>	TC <sub>2</sub>	TC <sub>4</sub>	TC <sub>2</sub>	TC <sub>4</sub>	TC <sub>2</sub>	TC <sub>4</sub>					
	42	15	45	22	32	14	31	13	29	12					
DC4	Bb1 (\$)		Bb2 (\$)		Bb3 (\$)		Dd1 (\$)		Dd2 (\$)		214	94	512		
	TC <sub>2</sub>	TC <sub>4</sub>	TC <sub>2</sub>	TC <sub>4</sub>	TC <sub>2</sub>	TC <sub>4</sub>	TC <sub>2</sub>	TC <sub>4</sub>	TC <sub>2</sub>	TC <sub>4</sub>					
	44	19	23	10	13	7	35	15	26	12					
DC5	Aa1 (\$)		Aa2 (\$)		Bb1 (\$)		Bb2 (\$)		Bb3 (\$)		245	141	590		
	TC <sub>2</sub>	TC <sub>4</sub>	TC <sub>2</sub>	TC <sub>4</sub>	TC <sub>2</sub>	TC <sub>4</sub>	TC <sub>2</sub>	TC <sub>4</sub>	TC <sub>2</sub>	TC <sub>4</sub>					
	40	21	48	25	24	12	13	6	10	5					

$\gamma_4 = 0.09$ ;  $\gamma_5 = 0.11$ . Regarding the algorithm parameters, many tests have been performed for TS-NSGA-II to calibrate the population size ( $pop_{size}$ ), the maximum number of iterations ( $gen_{max}$ ), the crossover probability ( $p_c$ ) and the mutation probability ( $p_m$ ). The calibrated parameters are as follows:  $pop_{size} = 150$ ,  $gen_{max} = 300$ ,  $P_s = 0.9$ ,  $P_c = 0.8$ ,  $P_m = 0.1$ . Let  $N = \{FDC1, FDC2, FDC3, FDC4, FDC5\}$  denote that each subset within  $S$  is a subset of  $N$  and represent a type of coalition.

Assuming all facilities agree to collaborate, a total of  $(2^5 - 1)$  coalition scenarios exist, excluding the null one. Note that A coalition can have a single participant. The optimization results for each coalition scenario are summarized in Table 13 and illustrated in Fig. 9.

In all scenarios, we observe a significant reduction in total cost and the number of vehicles when the network is optimized. For example, the grand coalition reduces the total cost from \$5162 to \$3030. In reality, this reduction in total cost must be distributed reasonably among logistics facilities, meaning that each participating logistics facility can benefit from the coalition.

The four types of costs – transportation cost (TC<sub>1</sub>), temperature control costs (TC<sub>2</sub>), penalty cost (TC<sub>3</sub>), and value losses (TC<sub>4</sub>), and the total cost (TC) for each facility are listed in Table 14. TC<sub>1</sub> and TC<sub>3</sub> in

Table 14 are the costs for each facility when a grand coalition {DC1, DC2, DC3, DC4, DC5} is formed and the CMFLDN is optimized, resulting in a total cost for all facilities of \$3030. TC<sub>2</sub> and TC<sub>4</sub> in each facility vary by product type and temperature control range, and are thus further decomposed. For instance, DC1 distributes five types of fresh product (i. e., Cc1, Cc2, Cc3, Dd1 and Dd2), which belong to two temperature control ranges in the grand coalition. TC<sub>2</sub> and TC<sub>4</sub> of fresh products Cc1 are \$31 and \$10, respectively. TC<sub>1</sub>, TC<sub>3</sub>, and the total cost at DC1 are \$202, \$71 and \$486, respectively.

5.4. Sensitivity analysis based on different temperatures

With everything else being equal, changes in the controlled temperature within the temperature control range will lead to opposite changes in TCC (TC<sub>2</sub>) and VL (TC<sub>4</sub>). Thus, we must balance TC<sub>2</sub> and TC<sub>4</sub> and find the equilibrium temperature that leads to the minimum sum of TC<sub>2</sub> and TC<sub>4</sub>. Fresh products Aa1, Bb1, Cc1 and Dd1 with four temperature control ranges (−20 °C)–(−15 °C), (−13 °C)–(−8 °C), (−5 °C)–(0 °C), and (1 °C)–(5 °C), respectively are selected for analysis. Eqs. (32) and (34) are respectively applied to calculate  $g_{mw}$  and COP, and thus TC2

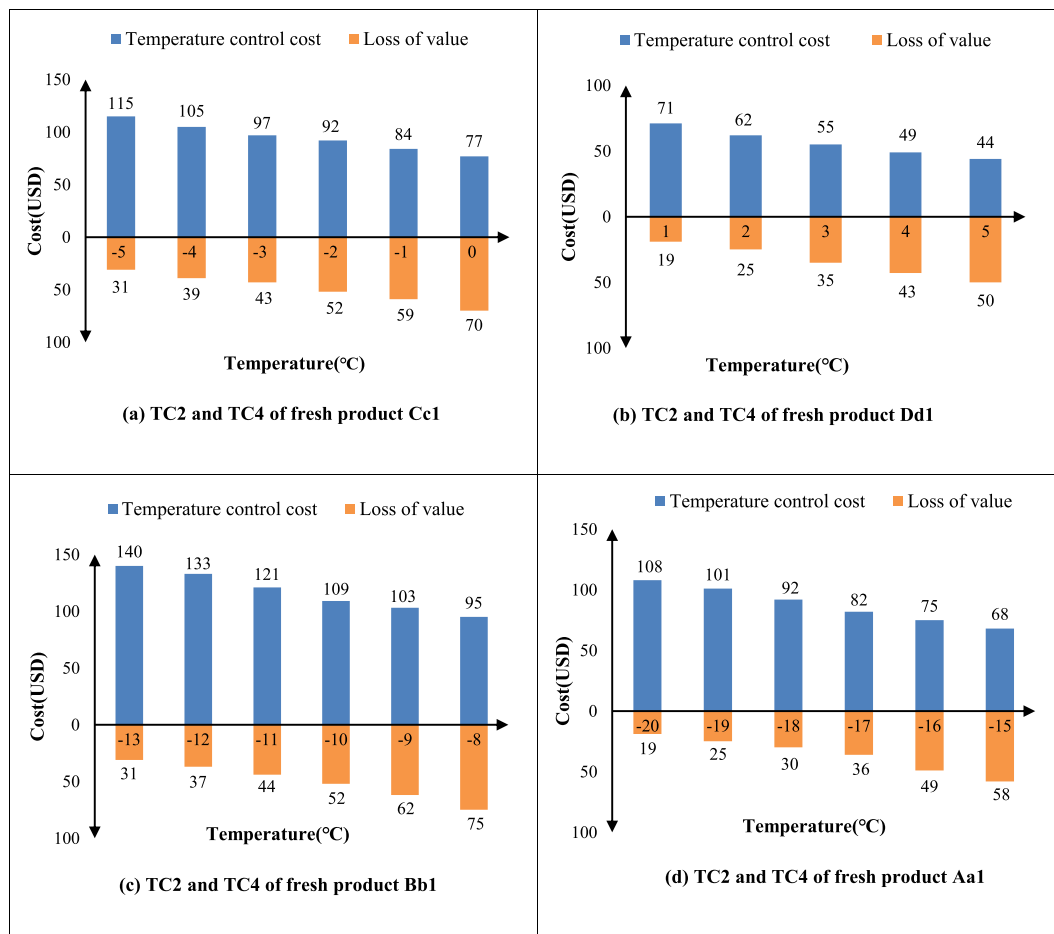


Fig. 10. Temperature control cost and loss of value of different fresh products.

and TC4 at different temperatures. The controlled temperature of the refrigerated vehicle is set to vary in the corresponding temperature control ranges, and the variations of TC<sub>2</sub> and TC<sub>4</sub> are shown in Fig. 10.

Fig. 10(a) indicates that low temperature leads to low TC<sub>4</sub> but high TC<sub>2</sub>, while high temperature leads to high TC<sub>4</sub> but low TC<sub>2</sub>. As any temperature within the temperature control range can satisfy the consumer’s demand for product freshness, an optimal control temperature for product Cc1 exists. The same is true for fresh products Dd1, Bb1, and Aa1 as shown in Fig. 10(b)–(d), respectively. The relationship between TC<sub>2</sub> and TC<sub>4</sub> for each fresh product is illustrated in Fig. 11.

In each sub-figure of Fig. 11, point B is optimal based on the Pareto-optimal principle (Tang et al., 2013; Pires et al., 2019). None of the remaining points (e.g., A or C) can satisfy the Pareto optimality. In Fig. 11(a), for example, -3°C is the best controlled temperature for distributing fresh product Cc1 at TCR (-5 °C)–(0 °C). Moreover, different scenarios that consider different controlled temperatures and whether facilities collaboration are explored for each TCR, and the comparison of the number of vehicles, number of time window violations, total delivery time, TCC, VL, and TLOC among these scenarios is summarized in Table 15.

Significant reductions in TCC, TLOC, and number of time window violations are observed in Table 15, when collaboration and the optimal controlled temperature are adopted. For example, the TLOC, TCC, and VL for fresh products Cc1, Cc2, and Cc3 with a controlled temperature of -5°C decrease to \$1202, \$353, and \$185 from \$1628, \$502, and \$211, respectively, when the FLDN changes from non-collaborative to collaborative network. In the collaborative network, the three costs can be further reduced to \$1032, \$270, and \$122 from \$1202, \$353, and \$185, respectively when optimal controlled temperatures (-3 °C, -1°C,

and -2 °C for fresh products Cc1, Cc2, and Cc3, respectively) are adopted. The results demonstrate that reasonable temperature control design and the collaborative mechanism play an important role in reducing the total logistics operational cost and loss of product values.

### 5.5. Analysis and discussion

#### 5.5.1. Comparison of different profit allocation methods

Game -theory-based methods are commonly used to allocate profit among participants (Wang et al., 2017b; Fernández et al., 2018). We apply the MCRS, the Shapley value model, the cost gap allocation model (CGA), and the equal profit method model (EPM) to obtain the optimal profit allocation plan in the grand coalition. The profit allocated to each of the five DCs affects the stability of the formed coalition. Therefore, the profit allocation scheme is optimized to promote long-term stable collaboration among logistics facilities. Table 16 shows the profit allocation using different allocation schemes.

According to snowball theory (Frisk et al., 2010; Lozano et al., 2013), the proximity of a profit allocation scheme to the core center determines the stability of the alliance under the allocation scheme. The scheme closest to the core center is the optimal profit allocation scheme and thus has the most stable alliance happen. According to Eq. (47), the core center is calculated as (368, 343, 408, 436, 449). Table 16 lists the resulting profit allocation schemes using the four methods, and the distance between each scheme and the core center. Compared with those of the other three methods, the result of MCRS is closest to the core center. Therefore, MCRS is identified as the best allocation method for fairly allocating profit among participants in the grand coalition.

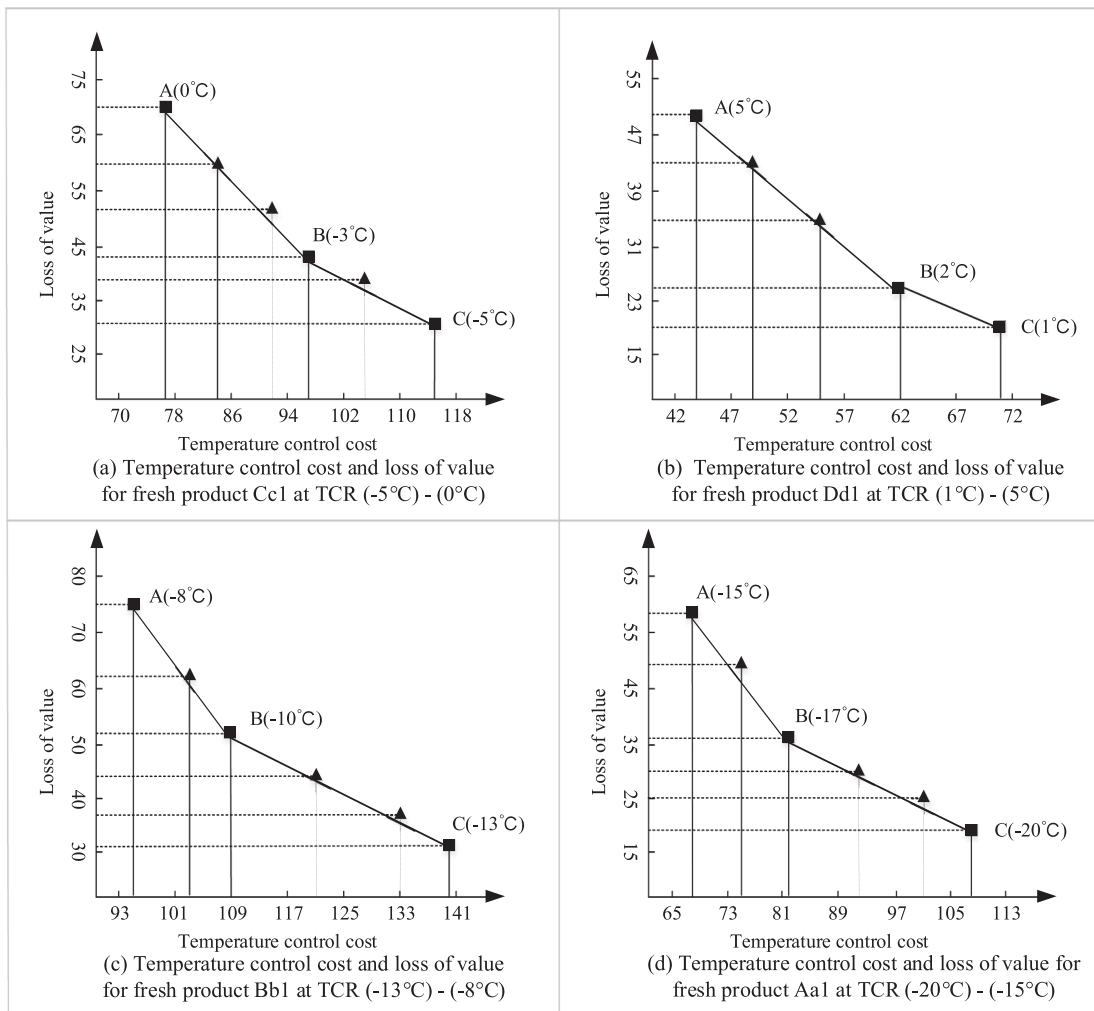


Fig. 11. Relationship between temperature control cost and loss of value for fresh products Cc1, Dd1, Bb1, and Aa1.

5.5.2. MCRS model application and coalition sequence selection

In practice, an alliance’s appeal to logistics facilities depends on whether the logistics facilities derive profit from the network operation as the operation strategies of most logistics companies are financially driven. The assumed minimum savings during the whole service time period to motivate an LSP to join an alliance is 6% of total cost saved. In other words, the coordination requirement is set to  $\chi = 0.06$ . Combining the aforementioned model and the optimization algorithm, the cost saving for a LSP is calculated as the gap between the total costs in the initial and optimized networks. Table 17 summarizes the profit allocation results for all non-empty coalitions using the MCRS model.

When DC1, DC2, DC3, DC4, and DC5 operate independently within one service time period, they can earn \$96, \$75, \$110, \$93, and \$101, respectively. In the grand coalition, their profits increase to \$372, \$340, \$418, \$429 and \$445. The result indicates that a grand alliance not only increases the total profit, but also benefits each alliance participant. In this paper, we assume that logistics facilities DC3 and DC4 are tied together regardless of the alliance is formed. The cost reduction percentages for all possible coalition formation sequences are shown in Fig. 12.

The stability of the grand alliance is studied by looking at whether existing alliance members can continuously benefit from new members joining the alliance. The benefit for a DC is measured by the cost reduction percentage calculated using Eq. (46) when a new member joins the alliance. In Fig. 12, the same final may have different coalition sequences, and the order in which each participant joins the coalition

affects the profit allocation and the coalition stability, thus affecting the long-term willingness of DCs to collaborate. We compare the optimal coalition sequences starting from DC1, DC2, DC3, and DC4 based on the SMP rule. The resulting cost reduction percentages for the DCs in each optimal coalition sequence are shown in Table 18.

The four coalition sequences satisfy the SMP shown in Table 18. Whenever a new logistics facility joins the alliance, the cost reduction percentages for existing members increase. The diagonal values of each table suggest that the best coalition sequence is  $\omega = \{DC3, DC4, DC1, DC5, DC2\}$ . The resulting best collaboration strategy is as follows. The cost for DC3 is reduced by 9.4% when it joins the coalition as the first member; DC4 subsequently joins the alliance, making the costs for DC3 and DC4 reduced by 22.0% and 22.4%, respectively; DC1 then enters the coalition, and DC3, DC4, and DC1 achieve cost reduction percentages of 31.1%, 28.0%, and 27.1%; DC5 participates as the fourth member and increases cost reductions to 32.6%, 34.4%, 31.6%, and 36.9%; and eventually, with the participation of DC2, the grand coalition is established. At this time, the costs for the five DCs are reduced by 35.6%, 39.1%, 36.5%, 45.5%, and 38.2%. This collaboration strategy ensures that every DC continuously benefits from collaboration, and thus prompts a strong willingness for each DC to collaborate with each other.

5.6. Management insights

The collaborative mechanism discussed above can effectively motivate multiple fresh logistics to join the collaborative alliance, and thus

**Table 15**  
Comparison of different temperature control ranges.

Temperature control range	Scenario	No. of refrigerated vehicles	No. of time window violations	Total delivery time (min)	TCC (\$)	VL (\$)	TLOC (\$)
Temperature control range (-5°C)-(0 °C)	Non-collaborative network for fresh products Cc1, Cc2, and Cc3 with -5°C, -5°C, and -5°C, respectively	7	7	82	502	211	1628
	Non-collaborative network for fresh products Cc1, Cc2, and Cc3 with 0 °C, 0 °C and 0 °C, respectively	7	7	81	439	265	1611
	Collaborative network for fresh products Cc1, Cc2, and Cc3 with -5°C, -5°C, and -5°C, respectively	7	2	66	353	185	1202
	Collaborative network for fresh products Cc1, Cc2, and Cc3 with 0 °C, 0 °C, and 0 °C, respectively	6	2	65	244	201	1129
	Collaborative network for fresh products Cc1, Cc2, and Cc3 with -3°C, -1°C, and -2°C, respectively	6	2	62	270	122	1032
	Collaborative network for fresh products Cc1, Cc2, and Cc3 with 0 °C, 0 °C, and 0 °C, respectively	6	2	62	270	122	1032
Temperature control range (1 °C)-(5 °C)	Non-collaborative network for fresh products Dd1 and Dd2 with 1 °C and 1 °C, respectively	6	8	69	391	118	1043
	Non-collaborative network for fresh products Dd1 and Dd2 with 5 °C and 5 °C, respectively	5	8	69	340	165	1004
	Collaborative network for fresh products Dd1 and Dd2 with 1 °C and 1 °C, respectively	5	3	55	125	48	511
	Collaborative network for fresh products Dd1 and Dd2 with 5 °C and 5 °C, respectively	5	3	54	95	77	494
	Collaborative network for fresh products Dd1 and Dd2 with 2 °C and 3 °C, respectively	5	2	52	117	52	455
	Collaborative network for fresh products Dd1 and Dd2 with 2 °C and 3 °C, respectively	5	2	52	117	52	455
Temperature control range (-13 °C)-(-8 °C)	Non-collaborative network for fresh products Bb1 and Bb2, and Bb3 with -13 °C, -13 °C, and -13 °C, respectively	6	4	75	416	217	1312
	Non-collaborative network for fresh products Bb1 and Bb2, and Bb3 with -8°C, -8°C, and -8°C, respectively	6	5	77	368	276	1379
	Collaborative network for fresh products Bb1 and Bb2, and Bb3 with -13 °C, -13 °C, and -13 °C, respectively	6	1	59	254	84	901
	Collaborative network for fresh products Bb1 and Bb2, and Bb3 with -8°C, -8°C, and -8°C, respectively	6	1	58	198	142	892
	Collaborative network for fresh products Bb1 and Bb2, and Bb3 with -10 °C, -12 °C, and -9°C, respectively	6	1	57	217	106	863
	Collaborative network for fresh products Bb1 and Bb2, and Bb3 with -10 °C, -12 °C, and -9°C, respectively	6	1	57	217	106	863
Temperature control range (-20 °C)-(-15 °C)	Non-collaborative network for fresh products Aa1 and Aa2 with -20 °C and -20 °C, respectively	7	5	64	428	186	1235
	Non-collaborative network for fresh products Aa1 and Aa2 with -15 °C and -15 °C, respectively	7	6	62	370	241	1289
	Collaborative network for fresh products Aa1 and Aa2 with -20 °C and -20 °C, respectively	6	2	50	229	62	734
	Collaborative network for fresh products Aa1 and Aa2 with -15 °C and -15 °C, respectively	6	2	50	153	115	705
	Collaborative network for fresh products Aa1 and Aa2 with -17 °C and -16 °C, respectively	6	2	49	175	83	680
	Collaborative network for fresh products Aa1 and Aa2 with -17 °C and -16 °C, respectively	6	2	49	175	83	680

**Table 16**  
Comparison of profit allocation methods.

Methods	Profit allocation schemes	Core center	Distance
Shapley	(386, 336, 424, 427, 431)	(368, 343, 408, 436, 449)	32
CGA	(348, 307, 419, 455, 475)		53
MCRS	(372, 340, 418, 429, 445)		14
EPM	(405, 317, 464, 392, 426)		87

lead to resource sharing and a reasonable temperature control design among fresh logistics facilities. This benefits the logistics network and the society from three aspects. First, it reduces the operational cost for not only the entire network, but also each logistics facility. Second, it decreases the value loss of perishable fresh products and thus improves customer satisfaction. Third, it reduces emissions from fresh logistics operation and leads to a more sustainable logistics. The management insights presented in this paper are summarized as follows.

*Resource sharing in fresh product distribution can effectively avoid the overlapping of delivery routes of long-distance transportation, and thus improve resource utilization in the CMFLDN.* Resource sharing enables the reallocation of limited resources based on customer demand characteristics, improving service synchronization and allowing logistics facilities to serve customers efficiently in the distribution of fresh products. In non-collaborative FLDNs, long-distance transportation, overlapping

delivery routes and empty truck backhaul resulting from the independent operation of logistics facilities leads to high TCC and VL in the fresh product distribution process. These problems can be solved by the rationalized allocation of limited resources among multiple FDCs and the reasonable division of time periods in a collaborative logistics network. Reduced transportation and temperature control costs also promote the sustainable development of urban fresh logistics.

*An optimal temperature control design method can effectively reduce the value loss of fresh products, and multi-center collaboration can improve the operation efficiency of FLDNs.* Different fresh products have different perishability and thus different temperature control and timeliness requirements. The freshness of fresh products, their value losses and thus the reliability of fresh products distribution service can be significantly improved by assigning each fresh product to a desired temperature control condition. This assignment is optimally implemented under resource sharing among multiple centers, which reduces the separate operation cost of FLDNs on temperature control and improves the stability and reliability of collaborative alliances. Therefore, an optimal temperature control design and a multicenter collaborative mechanism serve as the basis of a collaborative FLDN.

*The government and enterprises should leverage emerging technologies to promote collaboration and facilitate the sustainable development of the fresh logistics industry.* The government and logistics enterprises should continually optimize the layout of existing fresh logistics infrastructures,

**Table 17**  
Profit allocation results in collaborative FLDN.

$S$	$\sum_{n \in S} C_0(n)$	$C(S)$	$v^+(S)$	$\varphi(S, v^+)$
{DC1}	1019	917	96	(96; ■; ■; ■; ■)
{DC2}	891	811	75	(■; 75; ■; ■; ■)
{DC3}	1175	1058	110	(■; ■; 110; ■; ■)
{DC4}	1098	999	93	(■; ■; ■; 93; ■)
{DC5}	979	871	101	(■; ■; ■; ■; 101)
{DC1, DC4}	2117	1542	541	(278; ■; ■; 263; ■)
{DC1, DC5}	1998	1388	573	(284; ■; ■; ■; 289)
{DC2, DC4}	1989	1554	409	(■; 198; ■; 211; ■)
{DC2, DC5}	1870	1325	512	(■; 240; ■; ■; 272)
{DC3, DC4}	2273	1736	505	(■; ■; 259; 246; ■)
{DC3, DC5}	2154	1567	552	(■; ■; 272; ■; 280)
{DC1, DC2}	1910	1342	534	(281; 253; ■; ■; ■)
{DC1, DC3}	2194	1783	386	(190; ■; 196; ■; ■)
{DC2, DC3}	2066	1552	483	(■; 229; 254; ■; ■)
{DC4, DC5}	2077	1624	426	(■; ■; ■; 205; 221)
{DC1, DC2, DC4}	3008	2268	696	(231; 211; ■; 253; ■)
{DC1, DC2, DC5}	2889	2128	715	(233; 212; ■; ■; 271)
{DC1, DC3, DC4}	3292	2281	950	(277; ■; 366; 307; ■)
{DC1, DC3, DC5}	3173	2360	764	(221; ■; 287; ■; 256)
{DC2, DC3, DC4}	3164	2312	801	(■; 220; 316; 265; ■)
{DC2, DC3, DC5}	3045	2260	738	(■; 199; 285; ■; 254)
{DC1, DC4, DC5}	3096	2118	919	(280; ■; ■; 311; 329)
{DC2, DC4, DC5}	2968	2148	771	(■; 222; ■; 266; 283)
{DC3, DC4, DC5}	3252	2083	1099	(■; ■; 403; 338; 358)
{DC1, DC2, DC3}	3085	2171	859	(265; 244; 350; ■; ■)
{DC1, DC2, DC4, DC5}	3987	2570	1332	(316; 291; ■; 370; 354)
{DC1, DC3, DC4, DC5}	4271	2735	1444	(322; ■; 384; 378; 361)
{DC2, DC3, DC4, DC5}	4143	2650	1403	(■; 294; 379; 373; 357)
{DC1, DC2, DC3, DC4}	4183	2827	1275	(298; 274; 355; 348; ■)
{DC1, DC2, DC3, DC5}	4064	2685	1296	(306; 282; 365; ■; 343)
{DC1, DC2, DC3, DC4, DC5}	5162	3030	2004	(372; 340; 418; 429; 445)

formulate effective collaborative mechanisms and develop incentive measures to encourage fresh logistics enterprises to actively collaborate. Emerging information technologies such as the internet of things, big data, cloud computing, and blockchain bring opportunities to overcome obstacles to collaboration, and should be leveraged to encourage logistics enterprises to collaborate.

### 6. Conclusions

We study a vehicle routing problem with time windows and temperature control constraints in a collaborative FLDN and develop a solution algorithm for this optimization problem. First, extended k-means clustering is employed to reduce the computational complexity, and TS-NSGA-II is applied to optimize the CMFLDN composed of multiple FDCs and many customers. Then, a profit allocation method based on the MCRS model is proposed to allocate the benefits from the collaboration among FDCs. Finally, we find the optimal coalition sequence and discuss the stability of the alliance. In addition, we conduct temperature sensitivity analysis based on the principle of Pareto optimization.

The CMCVRP-RSTC is formulated as a bi-objective mixed-integer linear programming model to minimize the cost and number of vehicles under the time windows and temperature control constraints. The results of the case study on Chongqing show the comprehensiveness and high performance of the proposed solution algorithm. That is, the optimized CMCVRP-RSTC achieves a cost savings of \$2004. Meanwhile, the LSP plays an important role in facilitating the collaboration among FDCs. We explore profit allocation as a mechanism to motivate FDCs to collaborate. MCRS is selected to allocate profit over CGA, Shapley, and EPM. Alliance sequences and the profit allocation scheme affect the stability of a collaboration alliance. Finally, the best coalition sequence  $\omega = \{DC3, DC4, DC1, DC5, DC2\}$ , with respective allocated profits of \$372, \$340, \$418, \$429, and \$445 from the SMP rule is the most stable mechanism for the grand coalition.

The sensitivity analysis of controlled temperature indicates that the

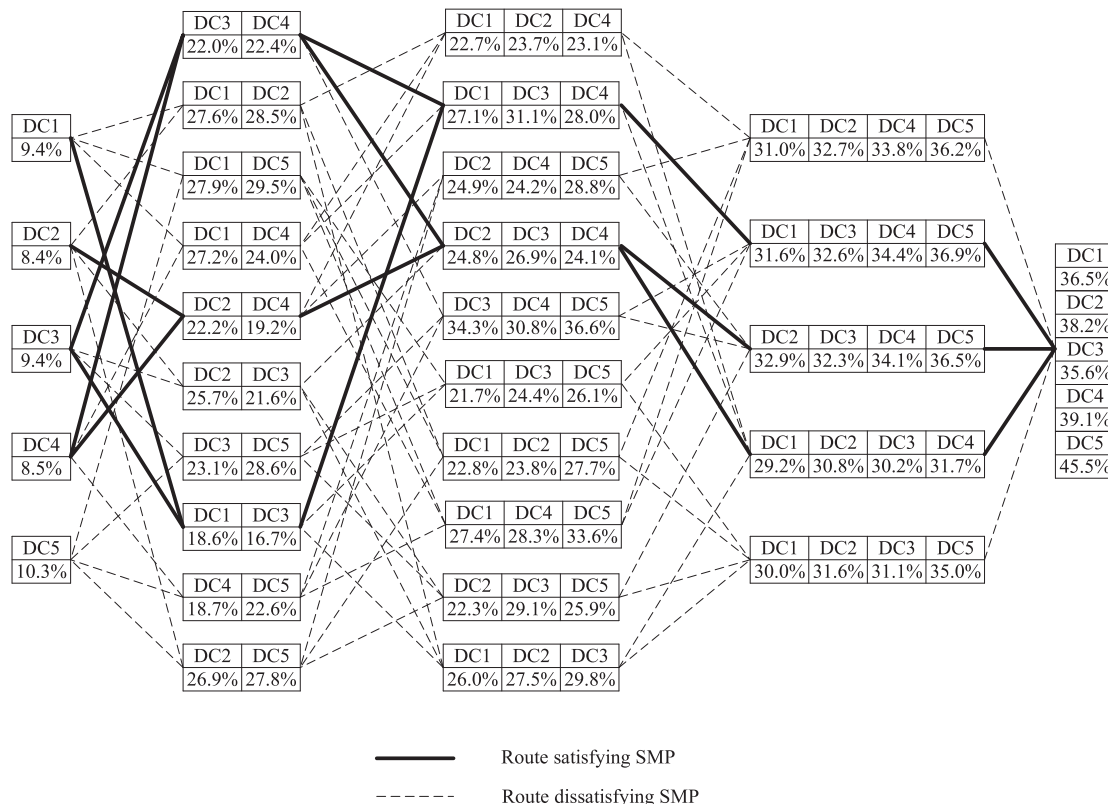


**Fig. 12.** Cost reduction percentages for all alliances.

**Table 18**  
Best sequential coalitions starting from D1 D2, D3, and D4 for SMP-based grand coalition.

$\omega_1 = \{DC1, DC3, DC4, DC5, DC2\}$						$\omega_2 = \{DC3, DC4, DC1, DC5, DC2\}$					
Player $n$	DC1	DC3	DC4	DC5	DC2	Player $n$	DC3	DC4	DC1	DC5	DC2
$\eta(n, \omega, 1)$	9.4%					$\eta(n, \omega, 1)$	9.4%				
$\eta(n, \omega, 2)$	18.6%	16.7%				$\eta(n, \omega, 2)$	22.0%	22.4%			
$\eta(n, \omega, 3)$	27.1%	31.1%	28.0%			$\eta(n, \omega, 3)$	31.1%	28.0%	27.1%		
$\eta(n, \omega, 4)$	31.6%	32.6%	34.4%	36.9%		$\eta(n, \omega, 4)$	32.6%	34.4%	31.6%	36.9%	
$\eta(n, \omega, 5)$	36.5%	35.6%	39.1%	45.5%	38.2%	$\eta(n, \omega, 5)$	35.6%	39.1%	36.5%	45.5%	38.2%
$\omega_3 = \{DC2, DC4, DC3, DC5, DC1\}$						$\omega_4 = \{DC4, DC3, DC1, DC5, DC2\}$					
Player $n$	DC2	DC4	DC3	DC5	DC1	Player $n$	DC4	DC3	DC1	DC5	DC2
$\eta(n, \omega, 1)$	8.4%					$\eta(n, \omega, 1)$	8.5%				
$\eta(n, \omega, 2)$	22.2%	19.2%				$\eta(n, \omega, 2)$	22.4%	22.0%			
$\eta(n, \omega, 3)$	24.8%	24.1%	26.9%			$\eta(n, \omega, 3)$	28.0%	31.1%	27.1%		
$\eta(n, \omega, 4)$	32.9%	34.1%	32.3%	36.5%		$\eta(n, \omega, 4)$	34.4%	32.6%	31.6%	36.9%	
$\eta(n, \omega, 5)$	38.2%	39.1%	35.6%	45.5%	36.5%	$\eta(n, \omega, 5)$	39.1%	35.6%	36.5%	45.5%	38.2%

TCC and VL of fresh products have a trade-off relationship. Sensitivity analysis highlights that environmental conditions must be considered when optimizing controlled temperature and evaluating all kinds of cost. Using the Pareto optimization method (Tang et al., 2013; Pires et al., 2019), we obtain the optimal controlled temperatures for fresh products Cc1, Dd1, Bb1, and Aa1 are  $-3^\circ\text{C}$ ,  $2^\circ\text{C}$ ,  $-10^\circ\text{C}$ , and  $-17^\circ\text{C}$ , respectively. The optimal controlled temperatures and effective collaboration are identified to be two critical factors affecting cost savings and the ability to meet freshness requirements for LSPs.

Compared with the existing research on optimizing multi-center FLDNs, our proposed approach has the following theoretical contributions. (1) Resource sharing and temperature control are both incorporated in a CMFLDN to obtain systematic optimization schemes. (2) A hybrid heuristic algorithm and a profit allocation method based on cooperative game theory are integrated into the CMCVRP-RSTC, optimizing vehicle scheduling, the control temperatures of various fresh products, and the profit allocations among FDCs. (3) A collaborative mechanism that facilitates the fair allocation of profits, stabilizes the collaborations, and ensures the reliability of the optimized CMFLDN is designed and tested. Therefore, studying the CMCVRP-RSTC can improve the efficiency and robustness of FLDNs, providing theoretical support for managing the operation of collaborative multi-echelon multiple-center fresh FLDNs, and propelling the sustainable development of the food supply chain and the construction of intelligent urban cold chain logistics distribution systems.

Future research can follow several directions. (1) An interesting topic is to consider the CMFLDN optimization problem with service time window assignment. (2) On the basis of combining the sharing of transportation vehicles and storage facilities, state-space-time

distribution network problems are also worth studying. (3) The integration of the pickup and delivery of fresh products in multi-service time periods is another prospective direction for future research. (4) The environmental impact of collaboration can be considered in model construction, which is a potential research direction for CMFLDNs.

**Declaration of Competing Interest**

The authors declare that they have no known competing financial interests or personal relationships that could have appeared to influence the work reported in this paper.

**Acknowledgments**

The authors would like to express our sincere appreciation for the valuable comments made by anonymous reviewers, which helped us to improve the quality of this paper. This research is supported by National Natural Science Foundation of China (Project No. 71871035, 71971036), Humanity and Social Science Youth Foundation of Ministry of Education of China (18YJC630189), Key Science and Technology Research Project of Chongqing Municipal Education Commission (No. KJQN202000723), Social Science Planning Foundation of Chongqing of China (No. 2019YBGL054) and Key Project of Human Social Science of Chongqing Municipal Education Commission (No. 20SKGH079). This research is supported by 2018 Chongqing Liuchuang Plan Innovation Project (cx2018111), Major Program of Key Disciplines in Dalian (2019J11CY002), and Chongqing Technology Foresight and System Innovation Project (cstc2020jsyj-zdxwtBX0003).

**Appendix A**

**Table A1**  
Basic information of customers' fresh product demands.

Customer	Time window	Demand	Product type	Product price	Temperature control range	Customer	Time window	Demand	Product type	Product price	Temperature control range
C1	[300 360]	18	Dd1	4	(1 °C)–(5 °C)	C76	[300 360]	25	Bb1	10	(-13 °C)–(-8 °C)
C2	[300 360]	16	Cc1	4	(-5 °C)–(0 °C)	C77	[300 360]	37	Dd1	4	(1 °C)–(5 °C)
C3	[300 360]	24	Dd1	4	(1 °C)–(5 °C)	C78	[200 500]	30	Dd1	4	(1 °C)–(5 °C)

(continued on next page)

Table A1 (continued)

Customer	Time window	Demand	Product type	Product price	Temperature control range	Customer	Time window	Demand	Product type	Product price	Temperature control range
C4	[300 360]	39	Dd1	4	(1 °C)–(5 °C)	C79	[200 500]	25	Bb1	10	(–13 °C)–(–8 °C)
C5	[300 360]	38	Cc1	4	(–5 °C)–(0 °C)	C80	[200 500]	22	Bb2	9	(–13 °C)–(–8 °C)
C6	[300 360]	29	Cc1	4	(–5 °C)–(0 °C)	C81	[200 340]	38	Bb3	8	(–13 °C)–(–8 °C)
C7	[300 360]	39	Cc2	5	(–5 °C)–(0 °C)	C82	[200 500]	18	Dd1	4	(1 °C)–(5 °C)
C8	[200 500]	39	Cc1	4	(–5 °C)–(0 °C)	C83	[200 500]	11	Dd2	5	(1 °C)–(5 °C)
C9	[200 500]	15	Cc3	7	(–5 °C)–(0 °C)	C84	[300 360]	33	Bb1	10	(–13 °C)–(–8 °C)
C10	[200 500]	34	Dd2	5	(1 °C)–(5 °C)	C85	[200 500]	24	Bb2	9	(–13 °C)–(–8 °C)
C11	[200 500]	29	Cc1	4	(–5 °C)–(0 °C)	C86	[300 360]	18	Bb3	8	(–13 °C)–(–8 °C)
C12	[200 500]	31	Dd1	4	(1 °C)–(5 °C)	C87	[300 360]	26	Dd1	4	(1 °C)–(5 °C)
C13	[200 500]	40	Cc2	5	(–5 °C)–(0 °C)	C88	[300 360]	14	Dd1	4	(1 °C)–(5 °C)
C14	[200 500]	35	Cc3	7	(–5 °C)–(0 °C)	C89	[200 500]	21	Dd1	4	(1 °C)–(5 °C)
C15	[200 500]	36	Dd2	5	(1 °C)–(5 °C)	C90	[200 350]	15	Bb2	9	(–13 °C)–(–8 °C)
C16	[300 360]	35	Cc3	7	(–5 °C)–(0 °C)	C91	[200 500]	36	Dd1	4	(1 °C)–(5 °C)
C17	[200 500]	40	Dd2	5	(1 °C)–(5 °C)	C92	[200 500]	34	Bb1	10	(–13 °C)–(–8 °C)
C18	[300 360]	36	Cc3	7	(–5 °C)–(0 °C)	C93	[200 500]	13	Dd1	4	(1 °C)–(5 °C)
C19	[300 360]	19	Dd2	5	(1 °C)–(5 °C)	C94	[200 500]	28	Bb2	9	(–13 °C)–(–8 °C)
C20	[300 360]	37	Dd2	5	(1 °C)–(5 °C)	C95	[300 360]	31	Dd2	5	(1 °C)–(5 °C)
C21	[300 460]	37	Cc3	7	(–5 °C)–(0 °C)	C96	[320 600]	17	Cc1	4	(–5 °C)–(0 °C)
C22	[200 500]	16	Cc3	7	(–5 °C)–(0 °C)	C97	[340 600]	35	Cc1	4	(–5 °C)–(0 °C)
C23	[200 500]	24	Cc1	4	(–5 °C)–(0 °C)	C98	[300 360]	16	Aa1	10	(–20 °C)–(–15 °C)
C24	[200 500]	23	Dd2	5	(1 °C)–(5 °C)	C99	[300 360]	30	Cc2	5	(–5 °C)–(0 °C)
C25	[200 500]	35	Dd2	5	(1 °C)–(5 °C)	C100	[300 360]	37	Aa1	10	(–20 °C)–(–15 °C)
C26	[200 500]	29	Cc2	5	(–5 °C)–(0 °C)	C101	[300 360]	30	Aa1	10	(–20 °C)–(–15 °C)
C27	[200 500]	19	Cc2	5	(–5 °C)–(0 °C)	C102	[300 360]	29	Cc2	5	(–5 °C)–(0 °C)
C28	[200 500]	16	Cc1	4	(–5 °C)–(0 °C)	C103	[300 360]	15	Aa2	7	(–20 °C)–(–15 °C)
C29	[200 500]	16	Bb1	10	(–13 °C)–(–8 °C)	C104	[300 360]	13	Cc2	5	(–5 °C)–(0 °C)
C30	[200 500]	18	Bb1	10	(–13 °C)–(–8 °C)	C105	[200 500]	32	Aa1	10	(–20 °C)–(–15 °C)
C31	[200 500]	31	Cc1	4	(–5 °C)–(0 °C)	C106	[200 500]	23	Aa2	7	(–5 °C)–(0 °C)
C32	[200 500]	28	Cc1	4	(–5 °C)–(0 °C)	C107	[200 500]	30	Aa1	10	(–20 °C)–(–15 °C)
C33	[200 500]	35	Bb1	10	(–13 °C)–(–8 °C)	C108	[200 500]	37	Cc3	7	(–5 °C)–(0 °C)
C34	[200 500]	20	Bb1	10	(–13 °C)–(–8 °C)	C109	[200 500]	39	Cc1	4	(–5 °C)–(0 °C)
C35	[200 500]	13	Bb2	9	(–13 °C)–(–8 °C)	C110	[200 500]	20	Cc1	4	(–5 °C)–(0 °C)
C36	[200 500]	33	Bb3	8	(–13 °C)–(–8 °C)	C111	[200 500]	30	Cc1	4	(–5 °C)–(0 °C)
C37	[200 500]	23	Cc1	4	(–5 °C)–(0 °C)	C112	[200 500]	37	Aa1	10	(–20 °C)–(–15 °C)
C38	[200 500]	20	Bb2	9	(–13 °C)–(–8 °C)	C113	[310 360]	33	Cc1	4	(–5 °C)–(0 °C)
C39	[200 500]	10	Bb3	8	(–13 °C)–(–8 °C)	C114	[200 500]	22	Cc1	4	(–5 °C)–(0 °C)
C40	[200 500]	38	Bb2	9	(–13 °C)–(–8 °C)	C115	[300 360]	30	Aa2	7	(–20 °C)–(–15 °C)
C41	[200 500]	26	Bb3	8	(–13 °C)–(–8 °C)	C116	[300 360]	31	Cc1	4	(–5 °C)–(0 °C)
C42	[200 500]	20	Bb3	8	(–13 °C)–(–8 °C)	C117	[300 360]	33	Aa2	7	(–20 °C)–(–15 °C)
C43	[200 500]	30	Cc1	4	(–5 °C)–(0 °C)	C118	[300 360]	36	Aa1	10	(–20 °C)–(–15 °C)
C44	[200 500]	25	Bb1	10	(–13 °C)–(–8 °C)	C119	[300 360]	28	Cc1	4	(–5 °C)–(0 °C)
C45	[200 500]	26	Bb1	10	(–13 °C)–(–8 °C)	C120	[300 360]	29	Aa1	10	(–20 °C)–(–15 °C)
C46	[200 500]	26	Bb1	10	(–13 °C)–(–8 °C)	C121	[300 360]	36	Aa2	7	(–20 °C)–(–15 °C)
C47	[200 500]	17	Cc2	5	(–5 °C)–(0 °C)	C122	[300 360]	34	Aa2	7	(–20 °C)–(–15 °C)

(continued on next page)

**Table A1** (continued)

Customer	Time window	Demand	Product type	Product price	Temperature control range	Customer	Time window	Demand	Product type	Product price	Temperature control range
C48	[200 500]	27	Bb1	10	(-13 °C)-(-8 °C)	C123	[300 360]	21	Cc1	4	(-5 °C)-(0 °C)
C49	[360 420]	18	Bb2	9	(-13 °C)-(-8 °C)	C124	[200 500]	22	Bb1	10	(-13 °C)-(-8 °C)
C50	[300 360]	33	Cc2	5	(-5 °C)-(0 °C)	C125	[300 360]	12	Aa1	10	(-20 °C)-(-15 °C)
C51	[300 360]	14	Cc2	5	(-5 °C)-(0 °C)	C126	[300 360]	11	Aa2	7	(-20 °C)-(-15 °C)
C52	[200 500]	35	Bb2	9	(-13 °C)-(-8 °C)	C127	[300 360]	21	Bb2	9	(-13 °C)-(-8 °C)
C53	[200 500]	37	Bb2	9	(-13 °C)-(-8 °C)	C128	[310 500]	27	Bb3	8	(-13 °C)-(-8 °C)
C54	[300 360]	40	Cc2	5	(-5 °C)-(0 °C)	C129	[320 360]	18	Aa1	10	(-20 °C)-(-15 °C)
C55	[200 500]	39	Bb3	8	(-13 °C)-(-8 °C)	C130	[320 500]	28	Aa2	7	(-20 °C)-(-15 °C)
C56	[300 360]	13	Cc3	7	(-5 °C)-(0 °C)	C131	[320 500]	31	Bb1	10	(-13 °C)-(-8 °C)
C57	[300 360]	20	Cc3	7	(-5 °C)-(0 °C)	C132	[320 500]	18	Bb2	9	(-13 °C)-(-8 °C)
C58	[200 500]	39	Cc3	7	(-5 °C)-(0 °C)	C133	[320 500]	37	Aa1	10	(-20 °C)-(-15 °C)
C59	[200 500]	15	Cc1	4	(-5 °C)-(0 °C)	C134	[320 500]	32	Bb2	9	(-13 °C)-(-8 °C)
C60	[200 500]	28	Bb2	9	(-13 °C)-(-8 °C)	C135	[290 500]	25	Aa1	10	(-20 °C)-(-15 °C)
C61	[200 500]	29	Cc1	4	(-5 °C)-(0 °C)	C136	[290 500]	17	Bb1	10	(-13 °C)-(-8 °C)
C62	[200 500]	40	Cc1	4	(-5 °C)-(0 °C)	C137	[290 500]	13	Aa1	10	(-20 °C)-(-15 °C)
C63	[300 360]	14	Bb2	9	(-13 °C)-(-8 °C)	C138	[290 500]	23	Aa2	7	(-20 °C)-(-15 °C)
C64	[300 360]	38	Bb3	8	(-13 °C)-(-8 °C)	C139	[290 500]	31	Aa2	7	(-20 °C)-(-15 °C)
C65	[200 350]	12	Dd1	4	(1 °C)-(-5 °C)	C140	[290 500]	25	Bb1	10	(-13 °C)-(-8 °C)
C66	[200 500]	31	Bb1	10	(-13 °C)-(-8 °C)	C141	[290 500]	28	Bb1	10	(-13 °C)-(-8 °C)
C67	[200 500]	32	Dd2	5	(1 °C)-(-5 °C)	C142	[290 500]	26	Bb1	10	(-13 °C)-(-8 °C)
C68	[200 350]	15	Dd2	5	(1 °C)-(-5 °C)	C143	[290 500]	30	Aa2	7	(-20 °C)-(-15 °C)
C69	[200 500]	14	Bb1	10	(-13 °C)-(-8 °C)	C144	[290 500]	16	Bb3	8	(-13 °C)-(-8 °C)
C70	[200 500]	39	Dd2	5	(1 °C)-(-5 °C)	C145	[290 500]	21	Aa2	7	(-20 °C)-(-15 °C)
C71	[200 500]	36	Bb1	10	(-13 °C)-(-8 °C)	C146	[290 500]	14	Bb1	10	(-13 °C)-(-8 °C)
C72	[200 500]	34	Bb1	10	(-13 °C)-(-8 °C)	C147	[290 500]	12	Bb2	9	(-13 °C)-(-8 °C)
C73	[300 360]	18	Bb1	10	(-13 °C)-(-8 °C)	C148	[290 500]	29	Aa2	7	(-20 °C)-(-15 °C)
C74	[200 500]	34	Bb1	10	(-13 °C)-(-8 °C)	C149	[290 500]	22	Aa1	10	(-20 °C)-(-15 °C)
C75	[300 360]	40	Dd2	5	(1 °C)-(-5 °C)	C150	[290 500]	14	Bb3	8	(-13 °C)-(-8 °C)

**Table A2**  
FDCs' service time windows.

FDC	Time window
DC1	[300 1000]
DC2	[300 1000]
DC3	[300 1000]
DC4	[300 1000]
DC5	[300 1000]

**References**

Abbasi, M., & Nilsson, F. (2016). Developing environmentally sustainable logistics: Exploring themes and challenges from a logistics service providers' perspective. *Transportation Research Part D: Transport and Environment*, 46, 273-283.

Amorim, P., & Almada-Lobo, B. (2014). The impact of food perishability issues in the vehicle routing problem. *Computers & Industrial Engineering*, 67, 223-233.  
 Arora, R., Kaushik, S. C., Arora, R., Lund, H., & Kaiser, M. J. (2015). Multi-objective and multiparameter optimization of two-stage thermoelectric generator in electrically series and parallel configurations through NSGA-II. *Energy*, 91, 242-254.

- Alikar, N., Mousavi, M. S., Ghazilla, R. A. R., Tavana, M., & Oluju, E. U. (2017). Application of the NSGA-II algorithm to a multi-period inventory-redundancy allocation problem in a series-parallel system. *Reliability Engineering & System Safety*, 160, 1–10.
- Behrouz, A. N., & Alireza, A. N. (2017). A constructive heuristic for time-dependent multi-depot vehicle routing problem with time-windows and heterogeneous fleet. *Journal of King Saud University-Engineering Sciences*, 29(1), 29–34.
- China.com, 2016. The development of fresh e-commerce encounters the logistics bottleneck: high cost of cold chain and few facilities. Retrieved from <[http://www.china.com.cn/food/2016-06/05/content\\_38605431.htm](http://www.china.com.cn/food/2016-06/05/content_38605431.htm)> on June 05, 2016.
- Centobelli, P., Cerchione, R., & Esposito, E. (2017). Developing the WH2 framework for environmental sustainability in logistics service providers: A taxonomy of green initiatives. *Journal of Cleaner Production*, 165, 1063–1077.
- Chen, H. K., Hsueh, C. F., & Chang, M. S. (2009). Production scheduling and vehicle routing with time windows for perishable food products. *Computers & Operations Research*, 36(7), 2311–2319.
- Chen, T., Zhang, N. L., Liu, T. F., Poon, K. M., & Wang, Y. (2012). Model-based multidimensional clustering of categorical data. *Artificial Intelligence*, 176(1), 2246–2269.
- Crujssen, F., Cools, M., & Dullaert, W. (2007). Horizontal cooperation in logistics: Opportunities and impediments. *Transportation Research Part E: Logistics and Transportation Review*, 43(2), 129–142.
- Diabat, A., Jabbarzadeh, A., & Khosrojerdi, A. (2019). A perishable product supply chain network design problem with reliability and disruption considerations. *International Journal of Production Economics*, 212, 125–138.
- Deb, K., Pratap, A., Agarwal, S., & Meyarivan, T. (2002). A fast and elitist multiobjective genetic algorithm: NSGA-II. *IEEE Transactions on Evolutionary Computation*, 6(2), 182–197.
- Fahimullah, M., Faheem, Y., & Ahmad, N. (2019). Collaboration formation and profit sharing between software development firms: A shapley value based cooperative game. *IEEE Access*, 7, 42859–42873.
- Fernández, E., Roca-Riu, M., & Speranzad, G. M. (2018). The shared customer collaboration vehicle routing problem. *European Journal of Operational Research*, 265(3), 1078–1093.
- Frisk, M., Göthe-Lundgren, M., Jörnsten, K., & Rönnqvist, M. (2010). Cost allocation in collaborative forest transportation. *European Journal of Operational Research*, 205(2), 448–458.
- Guajardo, M., & Rönnqvist, M. (2015). Operations research models for coalition structure in collaborative logistics. *European Journal of Operational Research*, 240(1), 147–159.
- Govindan, K., Jafarian, A., Khodaverdi, R., & Devika, R. (2014). Two-echelon multiple-vehicle location-routing problem with time windows for optimization of sustainable supply chain network of perishable food. *International Journal of Production Economics*, 152, 9–28.
- Hsu, C. I., & Liu, K. P. (2011). A model for facilities planning for multi-temperature joint distribution system. *Food Control*, 22(12), 1873–1882.
- Hu, H. T., Zhang, Y., & Zhen, L. (2017). A two-stage decomposition method on fresh product distribution problem. *International Journal of Production Research*, 55(16), 4729–4752.
- Hellström, M., Tsvetkova, A., Gustafsson, M., & Wikström, K. (2015). Collaboration mechanisms for business models in distributed energy ecosystems. *Journal of Cleaner Production*, 102, 226–236.
- He, Z. S., Chen, Y. H., & Shang, Z. H. (2019). A novel wind speed forecasting model based on moving window and multi-objective particle swarm optimization algorithm. *Applied Mathematical Modelling*, 76, 717–740.
- Ju, C. K., & Mu, C. C. (2010). Developing an advanced Multi-Temperature Joint Distribution System for the food cold chain. *Food Control*, 21(4), 559–566.
- Keizer, M., Akkerman, R., Grunow, M., Bloemhof, J. M., Haijema, R., & Vorst, J. G. A. J. (2017). Logistics network design for perishable products with heterogeneous quality decay. *European Journal of Operational Research*, 262(2), 535–549.
- Kuo, R. J., Mei, C. H., Zulvia, F. E., & Tsai, C. Y. (2016). An application of a metaheuristic algorithm-based clustering ensemble method to app customer segmentation. *Neurocomputing*, 205, 116–129.
- Kimms, A., & Kozeletskiy, I. (2016). Core-based cost allocation in the cooperative traveling salesman problem. *European Journal of Operational Research*, 248(3), 910–916.
- Lai, M., Cai, X., & Li, X. (2017). Mechanism design for collaborative production-distribution planning with shipment consolidation. *Transportation Research Part E: Logistics and Transportation Review*, 106, 137–159.
- Lee, D. J., & Jeong, I. J. (2009). Regression approximation for a partially centralized inventory system considering transportation costs. *Computers & Industrial Engineering*, 56(4), 1169–1176.
- Li, J., Li, Y., & Pardalos, P. M. (2016). Multi-depot vehicle routing problem with time windows under shared depot resources. *Journal of Combinatorial Optimization*, 31(2), 515–532.
- Li, J., Wang, R. L. T. T., Lu, Z. X., & Pardalos, P. M. (2018). Benefit analysis of shared depot resources for multi-depot vehicle routing problem with fuel consumption. *Transportation Research Part D: Transport and Environment*, 59, 417–432.
- Li, S. Y., Wang, Z. W., Wang, X., Zhang, D. Z., & Liu, Y. J. (2019). Integrated optimization model of a biomass feedstock delivery problem with carbon emissions constraints and split loads. *Computers & Industrial Engineering*, 137, Article 106013.
- Lin, C. C., & Chang, C. H. (2018). Evaluating skill requirement for logistics operation practitioners: Based on the perceptions of logistics service providers and academics in Taiwan. *The Asian Journal of Shipping and Logistics*, 34(4), 328–336.
- Liu, F. G., & Zhang, Z. J. (2017). Adaptive density trajectory cluster based on time and space distance. *Physica A: Statistical Mechanics and its Applications*, 484, 41–56.
- Liu, S. S., & Papageorgiou, L. G. (2018). Fair profit distribution in multi-echelon supply chains via transfer prices. *Omega-The International Journal of Management Science*, 80, 77–79.
- Lozano, S., Moreno, P., Adenso-Díaz, B., & Algaba, E. (2013). Cooperative game theory approach to allocating benefits of horizontal cooperation. *European Journal of Operational Research*, 229(2), 444–452.
- Mesa-Arango, R., & Ukkusuri, S. V. (2015). Demand clustering in freight logistics networks. *Transportation Research Part E: Logistics and Transportation Review*, 81, 36–51.
- Ma, Z. J., Wu, Y., & Dai, Y. (2017). A combined order selection and time-dependent vehicle routing problem with time widows for perishable product delivery. *Computers & Industrial Engineering*, 114, 101–113.
- Markova, I., Varone, S., & Bierlaire, M. (2016). Integrating a heterogeneous fixed fleet and a flexible assignment of destination depots in the waste collection VRP with intermediate facilities. *Transportation Research Part B: Methodological*, 84(5), 256–273.
- Martínez-Puras, A., & Pacheco, J. (2016). MOAMP-Tabu search and NSGA-II for a real Bi-objective scheduling-routing problem. *Knowledge-Based Systems*, 112, 92–104.
- Narasimha, K. V., Kivelevitch, E., Sharma, B., & Kumar, M. (2013). An ant colony optimization technique for solving min-max Multi-Depot Vehicle Routing Problem. *Swarm and Evolutionary Computation*, 13, 63–73.
- Nguyen, C., Dessouky, M., & Toriello, A. (2014). Consolidation strategies for the delivery of perishable products. *Transportation Research Part E: Logistics and Transportation Review*, 69, 108–121.
- Özen, U., Sosić, G., & Slikker, M. (2012). A collaborative decentralized distribution system with demand forecast updates. *European Journal of Operational Research*, 216(3), 573–583.
- Özener, O. O., Ergun, Ö., & Savelsbergh, M. (2011). Lane-exchange mechanisms for truckload carrier collaboration. *Transportation Science*, 45(1), 1–17.
- Pires, V. F., Pombo, A. V., & Lourenço, J. M. (2019). Multi-objective optimization with post-pareto optimality analysis for the integration of storage systems with reactive-power compensation in distribution networks. *Journal of Energy Storage*, 24, Article 100769.
- Rahbari, A., Nasiri, M. M., Werner, F., Musavi, M., & Jolai, F. (2019). The vehicle routing and scheduling problem with cross-docking for perishable products under uncertainty: Two robust bi-objective models. *Applied Mathematical Modelling*, 70, 605–625.
- Schmitt, A. J., Sun, S. A., Snyder, L. V., & Shen, Z. J. (2015). Centralization versus decentralization: Risk pooling, risk diversification, and supply chain disruptions. *Omega-The International Journal of Management Science*, 52, 201–212.
- Solomon, M. (1987). Algorithms for the vehicle routing and scheduling problems with time window constraints. *Operations Research*, 35(2), 254–265.
- Song, B. D., & Ko, Y. D. (2016). A vehicle routing problem of both refrigerated- and general-type vehicles for perishable food products delivery. *Journal of Food Engineering*, 169, 61–71.
- Song, H. J., Kim, J. Y., Kim, B. S., & Koo, J. (2019). Development of a food temperature prediction model for real time food quality assessment. *International Journal of Refrigeration*, 98, 468–479.
- Stellingwerf, H. M., Kanellopoulos, A., Vorst, J. G. A. J., & Bloemhof, J. M. (2018). Reducing CO<sub>2</sub> emissions in temperature-controlled road transportation using the LDVRP model. *Transportation Research Part D: Transport and Environment*, 58, 80–93.
- Su, C., Shi, Y. M., & Dou, J. P. (2017). Multi-objective optimization of buffer allocation for remanufacturing system based on TS-NSGAI hybrid algorithm. *Journal of Cleaner Production*, 166, 756–770.
- Silvestrin, P. V., & Ritt, M. (2017). An iterated tabu search for the multi-compartment vehicle routing problem. *Computers & Operations Research*, 81, 192–202.
- Tang, X. F., Zhang, J., & Xu, P. (2013). A multi-objective optimization model for sustainable logistics facility location. *Transportation Research Part D: Transport and Environment*, 22, 45–48.
- Tijs, S. N., & Driessen, T. S. H. (1986). Game theory and cost allocation problems. *Management Science*, 32(8), 1015–1028.
- Vreš'ál, J., Strof, J., & Pavlů, J. (2012). Extension of SGTE data for pure elements to zero Kelvin temperature-A case study. *Calphad*, 37, 37–48.
- Winshang.com, 2018. The loss rate is as high as 30%, and the fresh supermarket can't escape the cost curve? Fresh Retail Market Status Survey. Retrieved from <<http://news.winshang.com/html/063/7022.html>> on April 12, 2018.
- Wang, Y., Assogba, K., Fan, J. X., Xu, M. Z., Liu, Y., & Wang, H. Z. (2019). Multi-depot green vehicle routing problem with shared transportation resource: Integration of time-dependent speed and piecewise penalty cost. *Journal of Cleaner Production*, 232, 12–29.
- Wang, Y., Ma, X. L., Lao, Y. T., & Wang, Y. H. (2014). A fuzzy-based customer clustering approach with hierarchical structure for logistics network optimization. *Expert Systems with Applications*, 41, 521–534.
- Wang, Y., Ma, X. L., Liu, M. W., Gong, K., Liu, Y., Xu, M. Z., & Wang, Y. H. (2017). Cooperation and profit allocation in two-echelon logistics joint distribution network optimization. *Applied Soft Computing*, 56, 143–157.
- Wang, Y., Ma, X. L., Li, Z. B., Liu, Y., Xu, M. Z., & Wang, Y. H. (2017). Profit distribution in collaborative multiple centers vehicle routing problem. *Journal of Cleaner Production*, 144, 203–219.
- Wang, Z. (2018). Delivering meals for multiple suppliers: Exclusive or sharing logistics service. *Transportation Research Part E: Logistics and Transportation Review*, 118, 496–512.
- Wang, X. P., Wang, M., Ruan, J. H., & Zhan, H. (2016). The multi-objective optimization for perishable food distribution route considering temporal-spatial distance. *Procedia Computer Science*, 96, 1211–1220.

- Wang, X., Yu, F. S., Pedrycz, W., & Yu, L. (2019). Clustering of interval-valued time series of unequal length based on improved dynamic time warping. *Expert Systems with Applications*, 125, 293–304.
- Wang, Y., Assogba, K., Liu, Y., Ma, X. L., Xu, M. Z., & Wang, Y. H. (2018). Two-echelon location-routing optimization with time windows based on customer clustering. *Expert Systems with Applications*, 104, 244–260.
- Wang, Y., Ma, X. L., Xu, M. Z., Liu, Y., & Wang, Y. H. (2015). Two-echelon logistics distribution region partitioning problem based on a hybrid particle swarm optimization-genetic algorithm. *Expert Systems with Applications*, 42(12), 5019–5031.
- Wang, Y., Zhang, S. L., Assogba, K., Fan, J. X., Xu, M. Z., & Wang, Y. H. (2018). Economic and environmental evaluations in the two-echelon collaborative multiple centers vehicle routing problem. *Journal of Cleaner Production*, 197, 443–461.
- Xiao, J., Lin, B. L., & Wang, J. X. (2018). Solving the train formation plan network problem of the single-block train and two-block train using a hybrid algorithm of genetic algorithm and tabu search. *Transportation Research Part C: Emerging Technologies*, 86, 124–146.
- Yildiz, B., & Savelsbergh, M. (2019). Provably high-quality solutions for the meal delivery routing problem. *Transportation Science*, 53(5), 1372–1388.
- Yu, H. H., Mu, C. C., & Cheng, L. C. (2017). Distribution planning for perishable foods in cold chains with quality concerns: Formulation and solution procedure. *Trends in Food Science & Technology*, 61, 80–93.
- Zhan, Y., Lu, J. S., & Li, S. Y. (2013). A Hybrid GA-TS algorithm for optimizing networked manufacturing resources configuration. *Applied Mathematics and Information Science*, 7(5), 2045–2053.